

$$a_b = \frac{I_{ba}}{I_{bi}} = \frac{a_2 \cdot t_3 \cdot (1 + r_1 \cdot t_2)}{1 - r_1 \cdot r_3 \cdot t_2^2} \quad (6.62)$$

To meet the requirement of thermodynamic equilibrium we have

$$t + r_f + a_f = 1 \quad \text{and} \quad t + r_b + a_b = 1 \quad (6.63)$$

This relation is sometimes referred to as Kirchoff's law and can be used to replace e.g. Eqs 6.61 and 6.62 in order to save some calculation work.

The above equations must first be determined for each of the *TE* and *TM* waves, then the averages give the final result for a non-polarised wave, e.g. the reflection is given by

$$r = 0.5 (r_{TE} + r_{TM}) \quad (6.64)$$

These averages can not be used in a multi pane window, in which case all panes must be taken into account before the average values are determined.

If the refraction indices vary with wavelength we then have to integrate over the solar spectrum, and by integration over the hemisphere the parameters for diffuse radiation can be found.

6.3.3 Multiple pane windows

Up to now, we have only dealt with single layers surrounded by semi-infinite media. We will now place two or more layers in a combination. The thickness of the layers and the gaps between them are assumed to be small compared to other dimensions so the assumption of infinite reflections is still valid.

For each layer, the above discussed reflection, absorption and transmission will now be referred to as single layer's parameters, thus for the layer *j* alone in its semi-infinite surrounding:

- $r_{f,j}$ = reflection of forward incident radiation
- $r_{b,j}$ = reflection of backward incident radiation
- $a_{f,j}$ = absorption of forward incident radiation
- $a_{b,j}$ = absorption of backward incident radiation
- t_j = transmission of forward or backward incident radiation

As noted above, these parameters should be those for *TE* or *TM* waves, not the average for non polarised radiation.

$$t_c = I_{f,N+1} / I_{f,1} \quad (6.68)$$

$$r_c = I_{b,1} / I_{f,1} \quad (6.69)$$

and the absorption in each layer by Eq 6.67 and

$$a_{c,j} = I_{a,j} / I_{f,1} \quad (6.70)$$

In order to avoid the operations in Eqs 6.68 - 6.70, $I_{f,1} = 1$ can be used as boundary condition.

Transmission through the combination is always symmetrical but reflection and absorption may depend on the direction. In these cases, the same method could be used again but with different boundary conditions.

In Method 2 another common technique is used. The two first layers are combined to a fictive layer with all reflections taken into account in a similar way as in a single layer. We get for this fictive layer

$$t'_1 = \frac{t_1 \cdot t_2}{1 - r_1 \cdot r_2} \quad (6.71)$$

$$r'_1 = r_1 \frac{r_2 \cdot t_1^2}{1 - r_1 \cdot r_2} \quad (6.72)$$

and for each layer under influence of the other layer

$$a'_1 = a_1 \left(1 + \frac{r_2 \cdot t_1}{1 - r_1 \cdot r_2} \right) \quad (6.73)$$

$$a'_2 = \frac{t_1 \cdot t_2}{1 - r_1 \cdot r_2} \quad (6.74)$$

In case of more layers, the first fictive layer is combined in the above way with next layer giving a new fictive layer containing three layers et cetera. However, the complexity in calculation of the absorption in each layer will grow quickly with the number of layers.

In Method 3 a quite different technique, suggested by Källblad, 1973, is to use Eqs 6.65 - 6.67 in a method well suited for computer calculation. Rewriting Eq 6.66 gives

$$I_{f,j} = (I_{f,j+1} - r_{b,j} I_{b,j+1}) / t_j \quad (6.75)$$

Starting by setting $I_{f,N+1}$ to an arbitrarily positive value and $I_{b,N+1} = 0$ we can use the Eqs 6.75, 6.65 and 6.67 in that order for $j = N, N - 1$ et cetera until we get $I_{f,1}, I_{b,1}$ and $I_{a,1}$. Finally we get the overall coefficients with the Eqs 6.68, 6.69 and 6.70.

In ASHRAE (1993), the above quantity is called solar heat gain and is used e.g. when defining the Shading Coefficient.

Most programs assume an empty room when any of the above methods are used, but in some programs a part of the transmitted radiation can be assumed as convective heat gain to the room air. This is an approximate way to treat radiation absorbed in furniture

6.4.2 Direct radiation

Many simulation programs treat the direct radiation within rooms in a simplified way. The simplest is to assume that all radiation transmitted through a window is diffused by curtains etc. This assumption was defended by that the programs were used to estimate cooling load at situations where curtains or blinds always were used. With this assumption, the direct radiation is treated as described above.

As for the diffuse radiation, user defined or calculated time independent factors describing the distribution of the direct radiation are sometimes used. Some programs also treat a part of the transmitted direct radiation as convective heat gain to the room air.

The above simplified methods may introduce great errors, especially as the distribution vary by the solar position. In order to get more accurate results, one must determine in which surfaces the direct radiation is absorbed.

The direct radiation transmitted through a window can primarily hit many surfaces in a building, eventually after transmission through openings or glazed parts of inner walls and doors. How much of the radiation that will hit a specific surface may be calculated in a similar way as shading for a window. For each inner surface, all other surfaces may be shading or partly transparent screens. Thus the primarily incident direct radiation on all surfaces can be determined.

Next problems are the treatment of the absorbed and reflected parts of the primarily hit. Normally the radiation is smoothed out over the whole surface and the reflected part is treated as a diffuse radiative source. This allows treatment of the reflected radiation in the same way as described above for the diffuse radiation. In many cases, this approximation is acceptable, especially if walls, floors and ceilings are divided into small parts.

Caution has to be taken in rooms with large areas having specular reflection, e.g. glazed parts. If the solar altitude is low, most of the direct radiation may be reflected and then transmitted out from the building. Assuming diffuse reflections in these cases may lead to the conclusion that most of the radiation will be absorbed in inner surfaces. However, if one wants to treat specular reflections, an elaborate direct tracing has to be

6.5 Solar processor in DEROB-LTH

6.5.1 Input data to the solar processor

DEROB-LTH uses a climate data file containing hourly values day by day for one year or a period of a year covering the whole period of simulation. Climate data for days preceding and following the simulation period is allowed.

To calculate the solar radiation the DEROB-LTH program needs the following types of input data:

Location of site and time of simulation:

- Latitude of the site , positive to the North and negative to the South of the equator (°)
- Day of the year
- Hour of the day

Hourly values for solar radiation :

- Normal solar radiation (W/m²)
- Diffuse solar and sky radiation on horizontal surface (W/m²)

6.5.2 Solar altitude and azimuth

The position of the sun is calculated for each hour of the day in the middle of each month of the simulation period. The position of the sun is described by

- solar altitude angle $\theta_h = 90 - \theta_z$
- solar azimuth angle θ_a

Consider a coordinate system whose origin coincide with the center of the earth, and its x-y plane describes the equational plane and its z-y plane coincide with the direction of the incoming solar radiation. In this coordinate system the earth rotates about the z axis.

The position of a point on the surface of the earth for a given hour of the day is given by

$$\hat{r} = r_a (\sin \Phi_l \cos \Phi_H \hat{i} + \sin \Phi_l \sin \Phi_H \hat{j} + \cos \Phi_H \hat{k}) \quad (6.78)$$

6.5.3 Incident solar radiation on exterior surfaces

The insolation of solar radiation on exterior surfaces is calculated from measured hourly values of normal solar radiation, I_{DN} , and diffuse solar and sky radiation on horizontal surface, I_{dh} .

The total insolation on exterior surfaces includes three different sources :

- direct solar radiation
- diffuse solar and sky radiation
- direct, diffuse and sky radiation reflected from the ground surface

The calculation of insolation of direct solar radiation is based on the fact that each surface in the building model is divided into a regular grid of 25 elements. To determine the insolation of direct solar radiation on a surface, each of its elements is tested for any obstruction, opaque or transparent, between the center of the grid element and the sun's position. This approximation is used to calculate an effective area, $A_{E,i}$, for each surface i . $A_{E,i}$ is defined as follows:

$$A_{E,i} = \left(\sum_j tr_{ij} \right) \cdot \cos \theta_i \cdot \Delta A_i \quad (6.86)$$

tr_{ij} = progressive transmission through all obstructions between the grid element and the sun's position. For an opaque obstruction like a shading wall $tr_{ij} = 0$.

θ_i = solar incident angle on surface i

ΔA_i = the true area of the grid element of surface i

The insolation of direct solar radiation, I_D , is calculated as

$$I_D = A_{E,i} \cdot I_{DN} / A_i \quad (6.87)$$

A_i = the true area of surface i

The insolation of diffuse solar and sky radiation, I_{d1} , is calculated as

$$I_{d1} = 0.5 \cdot (1 + \cos \theta_t) \cdot I_{dH} \cdot C_{\theta z} \quad (6.88)$$

θ_t = the tilt angle of the surface to horizontal

$C_{\theta z}$ = the direct cosine of the sun in the zenith direction

I_{dH} = diffuse radiation on a horizontal plane

The insolation of solar radiation on a transparent surface is transmitted in two ways depending on the presence of shading devices like curtains or not.

If no shading device is active the transmitted solar radiation includes both a diffuse and a direct component as follows :

$$I_{dt} = 0.92 \cdot t_c \cdot (I_{d1} + I_{d2}) \quad (6.94)$$

$$I_{Dt} = t_{ci} \cdot I_D \quad (6.95)$$

I_{dt} = the transmitted part of insolation of diffuse solar radiation (W/m²)

t_{ci} = the transmittance t_c adjusted for the angle of incidence (-)

I_{Dt} = the transmitted part of insolation of direct solar radiation (W/m²)

If shading device is active, the direct component is treated as a diffuse source and the transmitted solar radiation is calculated as follows :

$$I_{dDt} = 0.92 \cdot k_{ec} \cdot t_c \cdot (I_{d1} + I_{d2} + I_D) \quad (6.96)$$

k_{ec} = a reducing factor for shading device like curtains (-)

I_{dDt} = the transmitted part of insolation of diffuse and direct solar radiation (W/m²)

6.5.5 Internal solar distribution within a zone

Solar radiation taking part in the internal distribution in a zone emanate from two different types of loadings

- diffuse solar radiation transmitted through a transparent surface into the zone
- direct solar radiation transmitted into the zone and reflected at a surface

Both types of loadings will be distributed as a diffuse source as follows:

$$P_{eci} = \sum_j I_{lum,ij} \cdot S_j \quad (6.97)$$

$I_{lum,ij}$ = the illumination factor that describes the fraction of the radiation from the surface j that arrives at surface i after all the reflections have been accounted for. (m²)

S_j = the strength of the loading at surface j (W/m²)

P_{eci} = the radiation received by surface i (W)

6.6 Solar processor in FRES

FRES uses the method from ASHRAE Fundamentals (1985) for the calculation of solar altitude and azimuth from location, day and local time, and is not referred here.

For the calculation of direct and diffuse radiation, a method based upon the cloud cover factor is used, and it is briefly described below. Simple geometry for external shading is also available, and is not described in detail.

6.6.1 Input data to the solar processor

FRES needs data for the location and time to calculate the hourly solar position. For calculation of solar radiation, the cloud cover ($0 < N_{CC} < 10$) is input from a weather file or from a constant value (24-hour simulations). FRES gets cloud cover from a special weather data file, which must be specially produced for new locations. The current version of FRES cannot use measured values for global solar radiation directly.

6.6.2 Solar altitude and azimuth

The method is completely described in ASHRAE Fundamentals and needs no repetition here.

6.6.3 Incident solar radiation on exterior surfaces

On a cloudy day, the Cloud Cover Factor N_{CCF} (Kimura and Stephenson, 1969) is used. The total radiation $I_{H,c}$ on a horizontal surface on a cloudy day is expressed as

$$I_{H,c} = I_H \cdot N_{CCF} \quad (6.98)$$

where I_H is total radiation on a horizontal surface a clear day. N_{CCF} is the cloud cover factor and is expressed by

$$N_{CCF} = k_P + k_Q \cdot N_{CC} + k_R \cdot N_{CC}^2 \quad (6.99)$$

where k_P , k_Q and k_R are constants or dependent of time of year, and N_{CC} is cloud cover ($0 < N_{CC} < 10$). The value k_P is called "Clearness index" and is treated as a site-dependent constant input by the user. k_Q varies as a

6.6.4 Transmitted solar radiation

A window is modelled as a single surface with direct transmittance t_{dir} and equivalent absorptance a_{eq} . Equivalent absorptance is calculated from the values for total and direct transmittance found in the manufacturer's data for any multi-pane window construction.

The angular dependence of the absorptance and transmittance is modelled using the coefficients for DSA Glass (ASHRAE Fundamentals, 1985).

Transmitted and absorbed solar heat load is calculated for every facade of every window in the building model. Absorbed heat is added directly to the window surface. Transmitted heat to each room is summed for every window facing away from a window facade. In case of inner facades, the heat taken from windows with facades facing towards the room is subtracted. A warning is issued if more than 30% direct transmitted heat is subtracted (retransmitted).

Windows facing towards other rooms are treated as outer facades in this first step of the calculation. Reduction in incident radiation of inner facades due to other windows must be done manually by providing some constant shading. Room geometry must be individually modelled for each facade by specifying overhang, side-fins and front obstruction.

6.6.5 Internal solar distribution within a zone

The net transmitted heat load is distributed to the surfaces by two artificial reflections.

1. Net transmitted radiation is focused only to the opaque surfaces, and a fraction (specified for the room) is evenly must be taken to have big enough opaque surfaces. The rest is reflected. Default value of the absorptance factor is 0.7.
2. Net reflected from 1. is evenly distributed to all surfaces. Opaque surfaces absorb all heat, and windows absorb a fraction $1-TU$, where TU is the mean resulting direct transmittance for all windows. The rest is "lost" from the model. Re-transmittance at this stage leaves the model even for windows with inner facades.

6.7 Solar processor in SUNREP (TRNSYS)

SUNREP computes the distribution of solar radiation into a room. Another program, the solar processor, computes the solar energy entering the room through the windows.

The solar processor used for the Shoebox test (see section 6.10) is the solar processor of MODPAS, a thermal simulation program. This processor is derived from the TRNSYS processor, based on J.A.Duffie and W.A.Beckman (1974).

6.7.1 Input data to the solar processor

For calculation of the solar radiation the following data are used by the solar processor.

- θ_l = Latitude of the site (North positive) ($^{\circ}$)
- A_g = Surface albedo (-)
- N_d = The day of the year, the julian day (1 - 366) or the day of the month and the month
- H = The hour of the day (1 - 24)
- I_{DH} = Horizontal direct solar radiation (W/m^2)
- I_{dH} = Horizontal diffuse solar radiation (W/m^2)
- θ_v = South azimuth of the surface (South = 0, -90 = East, +90 = West) ($^{\circ}$)
- θ_t = Angle between the horizontal and the surface (the slope) ($^{\circ}$)
- S_c = Shading coefficient of the window glass (=1 for a clear 3 mm glass)

In the solar distribution program input data are needed for the room, windows, subdivisions of walls (panels) and obstructions.

The rooms are defined by the geometry and the front wall azimuth. The windows are defined by number, geometry and position in the walls. The glass can be transparent or partly translucent (diffusing glass).

The walls are defined by geometry and position. Each wall can be paneled to refine the distribution. Internal windows between zones can be treated as panels: they have a coefficient of absorption of 0.90 and a coefficient of specular reflection of 0.10. With these values the solar energy absorbed by the window is the sum of the energy absorbed by the glass (— 0.10) and the energy passing through the glass (— 0.90) and entering another room.

The surfaces for each wall and panel are defined by two coefficients: one coefficient of absorption of the light and one coefficient of specular reflection. A perfect diffusing surface has a specular reflection of zero.

θ_i = Angle of incidence of beam radiation on the surface ($^\circ$)

The direct and diffuse incident solar radiation is calculated as

$$I_{Di} = \text{MAX} (0 , \cos \theta_i / \cos \theta_z) \cdot I_{DH} \quad (6.117)$$

$$I_{di} = R_d \cdot I_{dH} + R_g \cdot (I_{DH} + I_{dH}) \quad (6.118)$$

where

I_{DH} = Horizontal direct solar radiation (W/m^2)

I_{dH} = Horizontal diffuse solar radiation (W/m^2)

I_{Di} = Incident direct solar radiation on the surface (W/m^2)

I_{di} = Incident diffuse solar radiation on the surface (W/m^2)

The ratios R_d and R_g are given by

$$R_d = 1 + \cos \theta_t / 2 \quad (6.119)$$

$$R_g = \rho \cdot (1 - \cos \theta_t / 2) \quad (6.120)$$

6.7.4 Transmitted solar radiation

The transmitted and absorbed solar radiation is calculated in accordance with Stephenson (1965).

For the direct solar radiation, we have

$$t_D = - 0.00885 + 2.71235 \cos \theta_i - 0.626062 (\cos \theta_i)^2 - 7.07329 (\cos \theta_i)^3 + 9.75995 (\cos \theta_i)^4 - 3.89922 (\cos \theta_i)^5 \quad (6.121)$$

$$a_D = - 0.01154 + 0.77674 \cos \theta_i - 3.94657 (\cos \theta_i)^2 + 8.57881 (\cos \theta_i)^3 - 8.38135 (\cos \theta_i)^4 + 3.0118 (\cos \theta_i)^5 \quad (6.122)$$

where

t_D = Direct solar transmittance: solar radiation through a single glass (clear 3 mm)

a_D = Direct solar absorptance: solar radiation absorbed in a single glass (clear 3 mm)

6.7.5 Internal solar distribution within a zone

The direct solar radiation distribution is computed for each wall, panel and window for each hour of a day. Generally the calculation is made for one day in the month. A typical computing gives the direct solar distribution of the middle day of the 12 months of a year and one diffuse solar distribution for the year (independent of the hour and the day).

The results can be stored in files. The solar distribution files can be integrated in thermal simulation programs. The thermal simulation program calculates, with its own solar processor, the solar energy entering the room through the windows. The program SUNREP only distributes this solar energy on the internal surfaces.

The windows are divided into a number of rectangular subsurfaces. Two different calculations are made: one each hour of each day for the direct radiation, one for the diffuse radiation.

For the direct solar radiation, all the rays are parallel, for the diffuse solar radiation an hemisphere (the sky) is divided in 208 elements (isotropic diffuse solar distribution).

The attenuation due to the angle of incidence of the sun rays on the window glass can be included (angle modifier factor: algorithms of Stephenson, see chapter 6.7.4)

The method of calculation is a simplified ray tracing technique. The intersection between a ray entering the room and an internal surface (walls, panels or opposite windows) is geometrically calculated (three-dimensional). The sun ray striking a surface is divided into three parts:

- the absorbed part
- the diffuse reflected part
- the specular reflected part

All the surfaces are considered as composite reflecting elements. The coefficient of absorption and the coefficient of specular reflection determine the three parts.

- compound reflection
- diffuse reflection
- specular reflection

The solar energy which is not absorbed by the first stroked surface is reflected diffusely on all the other internal surfaces and is reflected as a beam to one surface. The second reflection is always diffuse. The diffuse reflection is calculated with the method of the view factors between the stroked surface and the other internal surfaces.

6.8 Solar processor in TSBI3

6.8.1 Input data to the solar processor

Climate data to be used by TSBI3 must exist in a special binary format. Data supplied as ascii-files can be converted to this binary TSBI3-format by use of the TRYCVE program developed by the Danish Building Research Institute.

The climate must be described by hourly values, day by day for the whole year, or day by day for periods of the year. The extension of the climate file must be *.TRY.

For calculation of the solar radiation the following data are used by TSBI3:

Location of the site the climate data belongs to:

- Latitude of the location, θ_l ($^{\circ}$), positive to the North
- Longitude of the location, θ_g ($^{\circ}$), positive to the East
- Standard time meridian. (hours). positive to the East.

Data concerning solar irradiation:

- Direct radiation at normal incidence, I_{DN} (W/m^2)
- Diffuse sky radiation on horizontal, I_{dH} (W/m^2)
- Cloud cover (octas) scale 0-8 or fraction, N_c (-).

The radiation and cloud cover data used by TSBI3 can be calculated by the TRYCVE program from any pair of solar data of which one excludes the diffuse sky radiation and the other includes the diffuse radiation.

TSBI3 uses the cloud cover for determination of the distribution of the diffuse solar radiation.

6.8.2 Solar altitude and azimuth

The position of the sun in relation to the building to be simulated is calculated hour by hour for one day (the 3rd day) in each week of the year, according to algorithms by Lund (Lund, 1977). The position is described by the sun's height angle over the horizon and its azimuth, the angle from north of the sun's beam projection on the horizontal plane.

The equation of time is estimated for the relevant day number of the year from:

$$\cos \theta_\alpha = -(\sin \theta_l \cdot \cos \theta_d \cdot \cos \theta_{ts} + \cos \theta_l \cdot \sin \theta_d) / \cos \theta_h \quad (6.131)$$

The position of the sun is calculated for every half hour of the third day in each week of the year.

The times for sunrise and sunset are also calculated, as well as the optical solar height $\theta_{h,opt}$ in which the real solar height is adjusted for the refraction in the atmosphere, according to the following:

$$\text{For } \theta_h > -0.005 \text{ rad} \quad \theta_{h,opt} = \theta_h + 0.0000225 / (\theta_h + 0.23) \quad (6.132)$$

$\theta_{h,opt}$ is the optical solar height (rad)

θ_h is the solar height (rad)

6.8.3 Incident solar radiation on exterior surfaces

The *total solar irradiance* on a surface is regarded to consist of 3 contributions, i.e.:

direct solar radiation (from the sun), I_{DN}

radiation from the sky (diffuse sky radiation), I_{dH}

reflected radiation from the surface of the ground, I_{Ag}

The *direct solar radiation* on a sloping surface can be calculated from the radiation at normal incidence:

$$I_{D,\theta_i} = I_{DN} \cdot \cos \theta_i \quad (6.133)$$

$\cos \theta_i$ is the cosine to the angle of incidence, calculated from:

$$\cos \theta_i = \cos (\theta_\alpha - \theta_w) \cdot \cos \theta_h \cdot \sin \theta_t + \sin \theta_h \cdot \cos \theta_t \quad (6.134)$$

θ_α is the solar azimuth angle (°)

θ_w is the orientation of the surface (°)

θ_h is the solar height angle (°)

θ_t is the slope of the surface, measured from horizontal (°), tilt angle

When the optical solar height is negative, the direct radiation is set to zero.

The *diffuse radiation* on a sloping surface I_{d,θ_i} can be expressed (Petersen, 1982) in comparison with diffuse radiation on the horizontal I_{dH} , with a factor f :

$$I_{d,\theta_i} = f \cdot I_{dH} \quad (6.135)$$

For surfaces, the direct solar radiation is set to 0 at times (in half-hours) where the sun is positioned lower than the defined sky-line. For windows, the direct radiation is adjusted by the fraction of the window being in the shade of the shadow or sky-line.

Like all other "systems" in TSBI3 a shadow is connected to a *schedule* for which it is possible to describe variations in the shading coefficient over the day and over the year.

Building obstructions, *overhang and side fins* are specified, which can shade for solar irradiation on a window. It can be described as a horizontal overhang which juts out over the window or vertical side fins at the left hand or right hand side of the window (or both), seen from face 2 (i.e. normally from outside).

Data for overhang and side fins are used for calculation of shading of the direct and the diffuse radiation. During definition of overhangs, which are large in comparison with the dimensions of the glazing, uncertainty is increased regarding the calculated solar irradiation, amongst other things because it does not make allowance for reflection of radiation from the overhangs.

The *total solar irradiation* on exterior surfaces is the sum of the contributions from direct sun radiation, diffuse sky radiation, and radiation reflected from the ground, calculated from the expressions above:

$$I_{tot,\theta_i} = I_{D,\theta_i} + I_{d,\theta_i} + I_{Ag,\theta_i} \quad (6.142)$$

6.8.4 Transmitted solar radiation

The transmission of the direct solar radiation through windows is calculated (Johnsen and Grau, 1994) from the coefficient for transmission at normal incidence from:

$$f_{\theta_i} = f_{(\perp)} \cdot (1.0 - 0.04 \cdot (\theta_i/100) - 2.933 \cdot (\theta_i/100)^6 + 2.13 \cdot (\theta_i/100)^{12}) \quad (6.143)$$

$f_{(\perp)}$ is the transmission coefficient for direct solar radiation at normal incidence

θ_i is the angle of incidence (°)

The transmission of the diffuse solar radiation is simply calculated as

$$f_d = 0.9 \cdot f_{(\perp)} \quad (6.144)$$

f_d is the transmission coefficient for diffuse solar radiation

To surfaces is the part of the radiation distributed between the individual constructions in the floor, walls and ceiling. The total solar radiation is distributed according to a "distribution key" which expresses the relative solar intensity (W/m^2) to floor, walls and ceiling respectively.

The parameter "*max to other zones*" is only relevant for windows in internal walls, and is described in the following section.

6.8.6 Internal solar distribution between zones

The program calculates principally the solar radiation through a window in an internal wall, as if it were placed in an external wall. The solar radiation which strikes the window in the internal wall must first pass through the windows in the zone in front and often it is only a small part of the solar radiation to the first zone, which passes on. How great an amount will pass on is calculated on the basis of the following:

Size and orientation of the windows, transmittance for radiation through the windows in the outer wall and in the internal wall, as well as data for "overhang" and "side fins" around the internal window and the shadows from this.

A pre-requisite for the solar radiation being calculated with an acceptable accuracy is therefore that the geometric conditions and the total shading effect of the zone which lies in front of the internal window, can approach the effect of the overhang, side fins and shadows on the window. The ceiling in the zone in front must thus be described as an overhang over the internal window, the walls and side fins or shadows, whilst other shading elements, for example, minor wall surfaces, window bars etc., in the outer walls must be taken account of as a reduction in the total transmittance of solar radiation which both passes through the external zone and through the internal window.

Max to other zones is a parameter for definition of how great a part of the solar radiation in the current zone can as a maximum be assumed to pass through internal windows to adjacent zones.

Under certain conditions, the program can calculate the solar radiation through windows in internal walls. As this calculation of the solar radiation will often be encumbered with a relatively large uncertainty, this parameter is used to ensure that calculation errors do not lead to results which are physically impossible, for example, a zone which 'passes on' more solar energy than it receives itself.

When clipping polygons, two polygons are involved at a time. The polygon to be clipped is referred to as the *subject polygon* and the clipping polygon as the *clip polygon*. In the case of shadings on a window, the window is the subject polygon, and the shading polygon is the clip polygon.

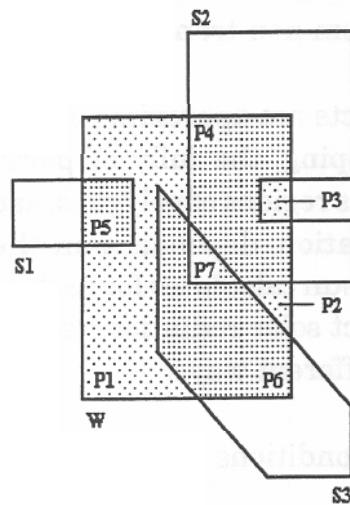


Figure 6.7 Region and polygons.

An area of a certain property, e.g. the radiated part(s) of a window, is referred to as *a region*. A region is described as a collection of zero, one or more non-overlapping polygons.

In Figure 6.7 the window polygon W is partly shaded by the convex polygons S1 and S3, and the concave polygon S2. If all the shadings are opaque, the resulting radiated region consists of the polygons P1, P2 and P3. However, if the shading polygons are transparent, the resulting radiated region consists of the polygons P1, P2, P3, P4, P5, P6 and P7.

The factor of transparency for a resulting polygon is the product of the factor of transparency of the overlapping polygons. The factor of transparency for P7, for example, will be the product of the factors of transparency for P4 and P6.

6.9.3 Application

An algorithm for clipping a concave polygon to the boundaries of another concave polygon has been developed in the context of hidden surface removal for applications in Computer Graphics (Weiler and Altherton, 1977) and (Rogers, 1985). The same algorithm can be used when determining shaded regions of windows or solar collectors.

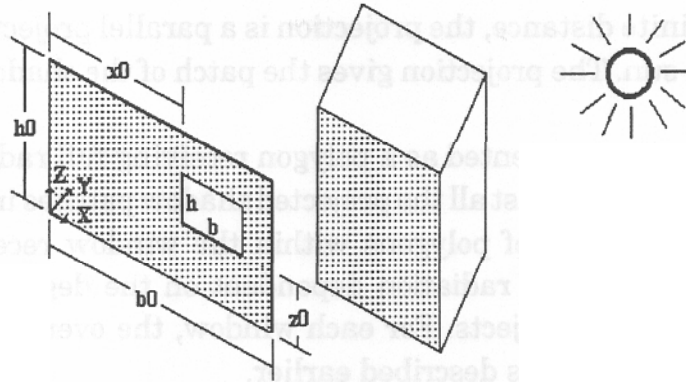


Figure 6.8 Coordinate system, definition of windows and shading objects.

3. Definition of the windows in the wall, i.e. the position of the windows in the wall and their shape. The window can be defined as any polygon or circular shape. The position of the window, as well as the overhang and side fins are defined according to the measures indicated in Figure 6.9. The overhang and side fins can be transparent in any degree.

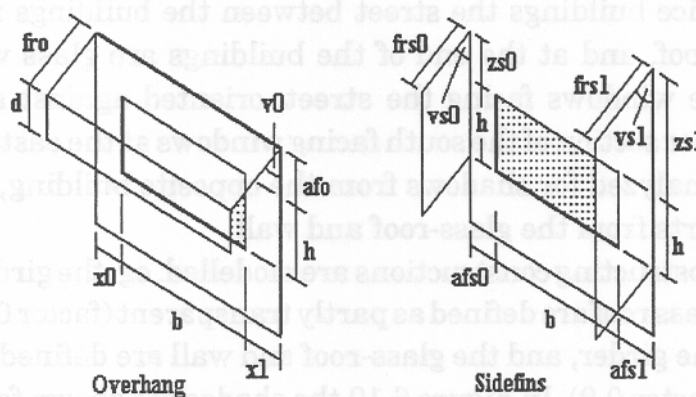


Figure 6.9 Definition of window overhang and sidefins.

4. Definition of remote shading objects. Each object is approximated by a number of plane polygons, each of which is attached with a factor of transparency. The polygons are defined in the chosen coordinate system, cf. Figure 6.8.

Calculation of incident solar radiation on windows is a complex problem to handle. It includes the following tasks:

First, the position of the sun is calculated for a certain day of the year at a given time. According to the sun's position, the shading objects are projected onto the surface with the windows (or solar collectors). As the

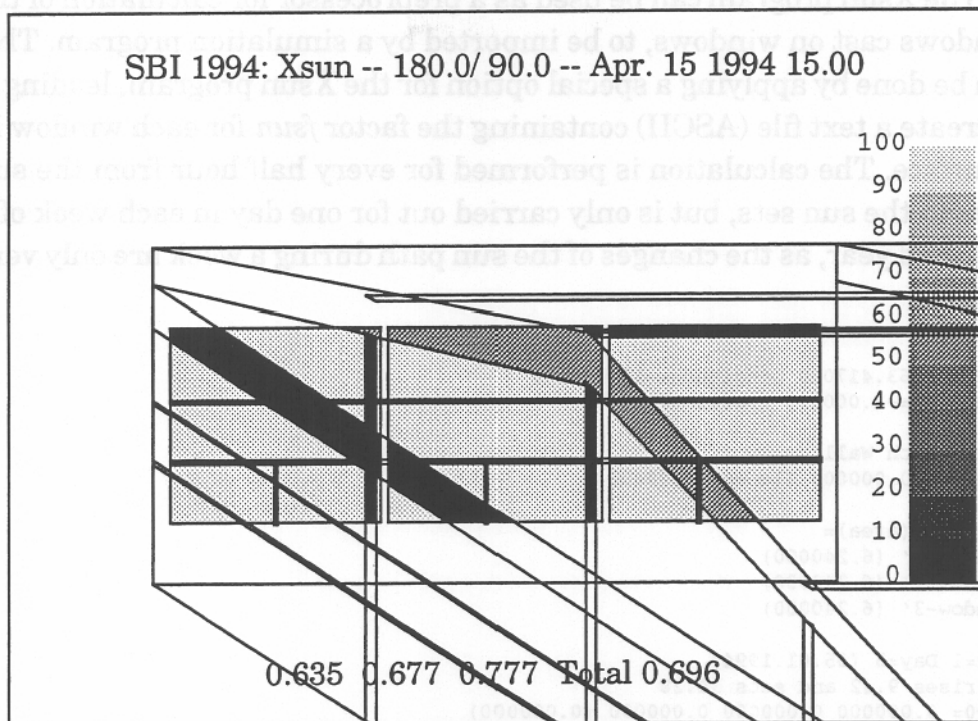


Figure 6.10 Shadings on windows in facades to overglassed street.

6.9.5 Shadow calculations for thermal simulation programs

In thermal simulation programs the calculation of shadows cast by exterior objects on the windows are often relatively crude. The same is the case for shadows caused by the surroundings nearby the windows, approximated by side fins and overhang. This, of course, also leads to inaccurate calculations of the direct solar irradiation on the windows, and thus, a crude prediction of the solar heat gains.

Many thermal simulation programs do not allow for definition of the surroundings in great detail, and therefore, implementation of more precise algorithms in the programs can not improve the precision of the shadow calculations without extending the data input considerably. However, by performing the shadow calculations through a detailed program, external to the simulation program, and later importing the results into a simulation program, a better precision without extending the data input needed for the simulation program can be obtained. Extending a simulation program with ability for importing a file is rather simple compared to extensions with more complicated input and implementation of new and more complicated calculation algorithms.

6.10 The shoebox study

This study was made in order to compare different methods of calculating the solar radiation and its distribution in a sunspace and a building connected to the sunspace. Calculations have been made for a simple room with two windows to the south and then for the same room combined with a sunspace in front of the south facade.

6.10.1 Description of the shoebox

The basic geometry of the studied building is the same as used in IEA Task 12B/Annex 21C, in the BESTEST study (Judkoff and Neymark). This building only consists of one room with two large windows to the south. The room is 48 m² and the windows are each 6 m² and double glazed, see Figure 6.12.

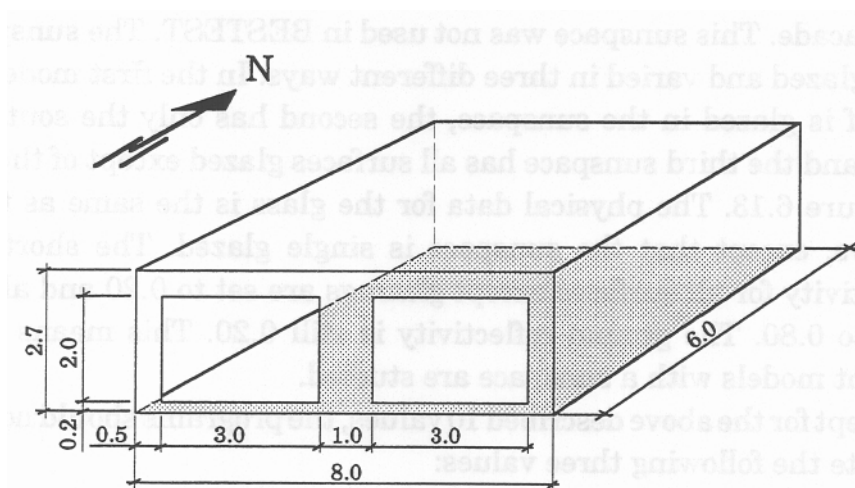


Figure 6.12 The shoebox.

The absorptivity of short wave radiation was set to 0.5 for all surfaces except glazings. Each pane of the window has the absorptance 0.06, reflectance 0.08 and transmittance 0.86 at perpendicular incidence. The ground reflectivity was set to 0.20.

The used simulation programs (FRES, DEROB-LTH, TSBI3 and TRNSYS/SUNREP) were to give hourly values of the following.

- P_{tot} total incoming short wave radiation to the outside of the windows (W)
- total short wave radiation transmitted to the room (W)
- P_{net} the part of P_{trans} that stays in the room. (%)

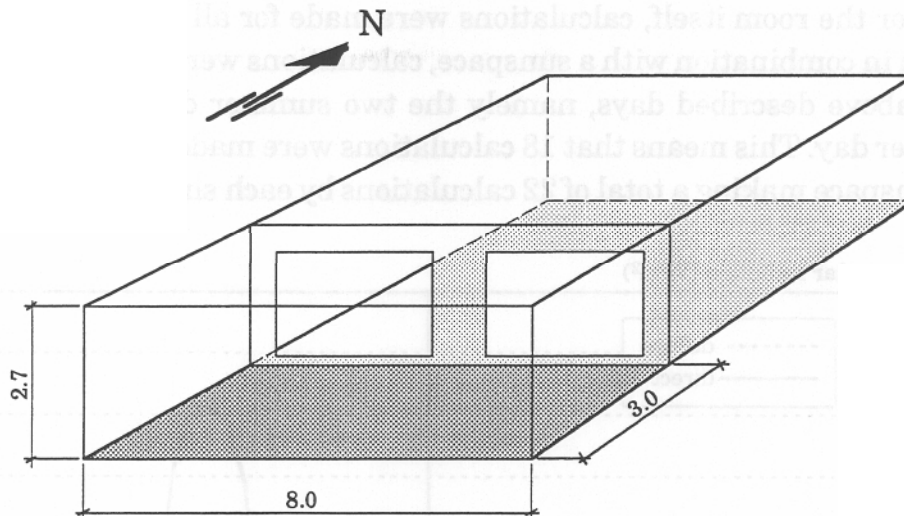


Figure 6.13 The shoebox with a sunspace.

A certain amount of solar radiation is hitting the outside of the sunspace. A part of this is transmitted into the sunspace, some of this is reflected out again, some passes through into the room behind and the rest is absorbed in the sunspace. A part of the radiation that is transmitted to the room is reflected out into the sunspace again and the rest is staying in the room. The net radiation is the part of the solar radiation that is staying in the sunspace, alternatively the room, and then used in the energy balance in order to calculate temperatures, energy needs and so on. In this study we are just comparing the calculation of the distribution of solar radiation to different volumes and surfaces. There are no calculations made of temperatures or energy needs.

6.10.3 Climatic data

Climatic data from Copenhagen, Denmark, is used, two winter days and two summer days from the Danish Test Reference Year (TRY). The latitude for Copenhagen is 56.0°N . One clear day and one overcast day were chosen for each season. The 19th and the 22nd of December are chosen as winter days, see Figure 6.14 showing the solar radiation. The 19th of December is a totally cloudy day with only diffuse solar radiation and the 22nd of December is a clear winter day. In Figure 6.15, the solar radiation in the overcast summer day (19th of May) and the clear summer day (7th of June), is shown.

6.10.4 Results for the shoebox without a sunspace

At the different programs first calculated the solar radiation hitting the two windows when no sunspace was placed in front of the building. The transmitted solar radiation and its distribution to different surfaces in the room were also calculated. Only some examples are shown in this chapter.

In Figure 6.16 the total solar radiation hitting the outside of the two windows during the clear winter day is shown. The sum of the total solar radiation hitting the windows during the day is 37.1 kWh according to TSBI3, 36.8 kWh with DEROB-LTH, 34.3 kWh with TRNSYS and 32.5 kWh with FRES.

In Figure 6.17 the transmitted solar radiation is shown. The transmitted radiation is 27.3 kWh calculated with TSBI3, 27.2 kWh by DEROB-LTH, 26.3 kWh by TRNSYS and 25.0 kWh by FRES during the clear winter day.

When the weather is clear, that is when the solar radiation contains both a direct and diffuse part of radiation, the part of solar radiation hitting a specific surface in a room will vary during the day. In Figure 6.18 the part of the transmitted solar radiation hitting the floor in the room during the clear winter day is shown. The four different programs estimate that about 25-35% of the transmitted solar radiation will hit the floor. TSBI3 and FRES have constant values during the day and TRNSYS/SUNREP and DEROB-LTH have hourly variations. The part that hits the west wall in the room is shown in Figure 6.19. The difference between the programs is considerable. The solar radiation will directly hit the west wall in the morning and the east wall in the afternoon. Note that in TSBI3, the distribution factors are input data, i.e. they are defined by the user.

During the clear summer day, the solar radiation is more intense. However, as the sun in the middle of the day is higher up in the sky, the resulting incident radiation to the vertical windows is not higher than in the middle of the winter day. The total incident radiation during a day is however much higher in the clear summer day than in the winter day, as the sun is shining several more hours per day. In Figure 6.20 the total solar radiation hitting the outside of the windows is shown. In this case, TRNSYS and DEROB-LTH give almost the same results, TRNSYS 55.0 kWh during the day and DEROB-LTH 54.4 kWh. TSBI3 gives the highest value, 58.4 kWh and FRES the lowest, 49.6 kWh. There is also a time difference of 1 hour between TSBI3 and the other programs, which also is seen in other calculation cases.

The transmitted radiation is shown in Figure 6.21 and here TRNSYS is the highest with 37.0 kWh, TSBI3 35.6 kWh, DEROB-LTH 34.7 kWh and FRES 34.3 kWh.

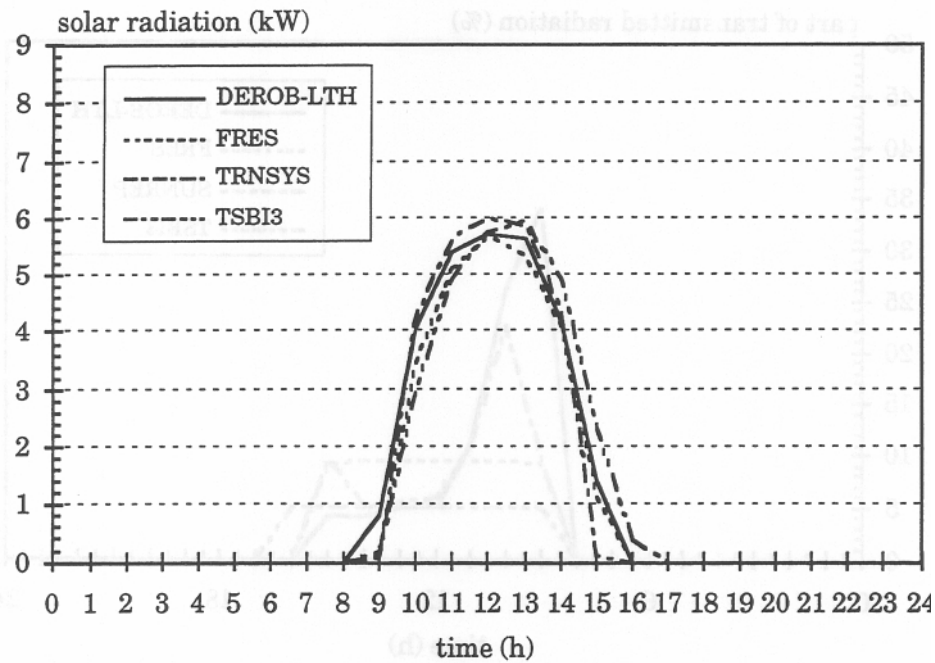


Figure 6.17 Transmitted solar radiation through the two windows during the clear winter day.

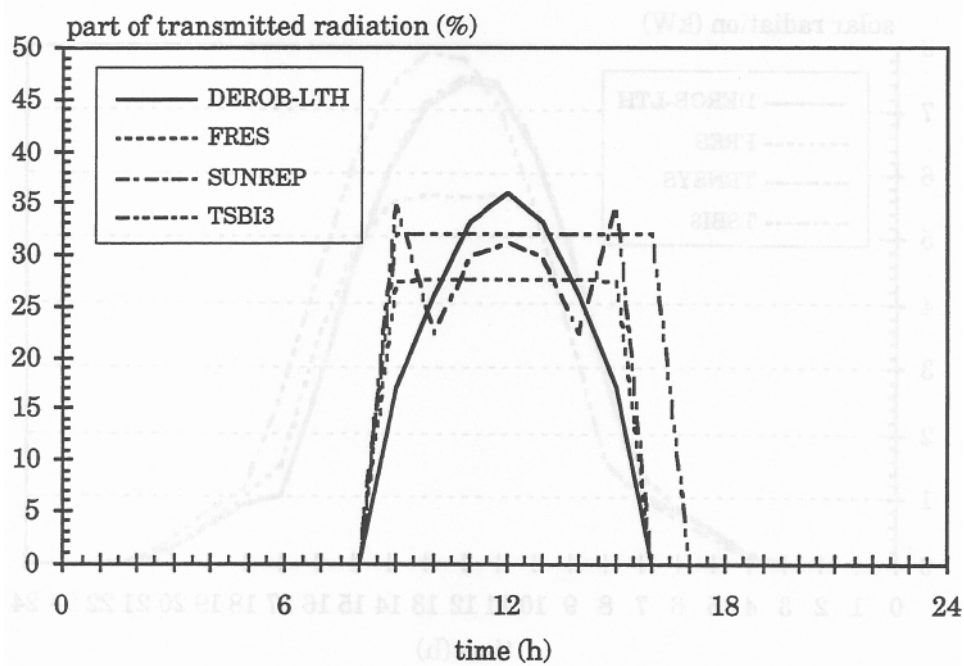


Figure 6.18 Part of the transmitted radiation hitting the floor of the shoebox during the clear winter day.

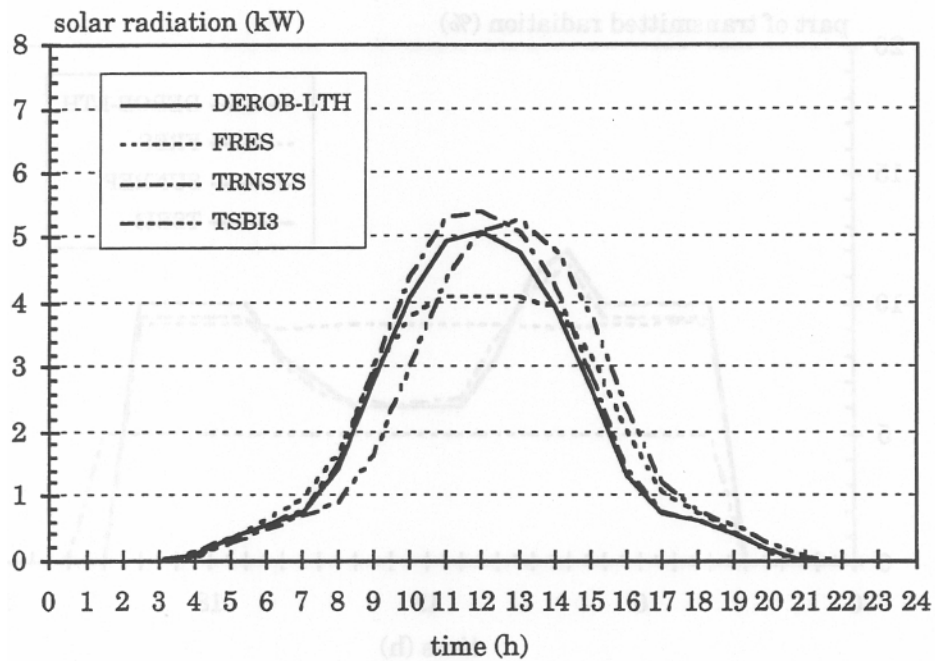


Figure 6.21 Transmitted solar radiation through the two windows during the clear summer day.

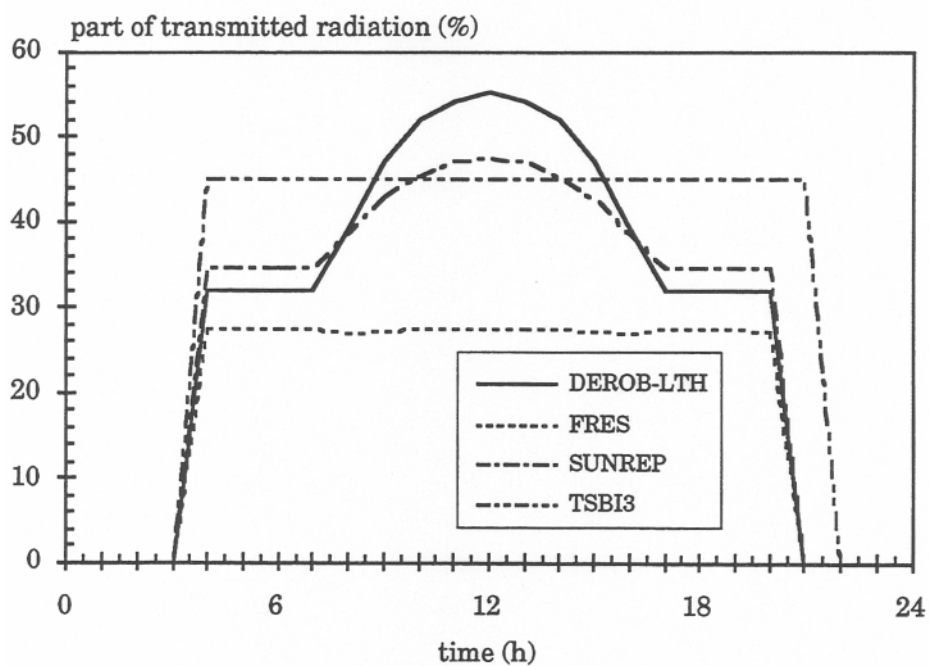


Figure 6.22 Part of the transmitted radiation hitting the floor of the shoebox during the clear summer day.

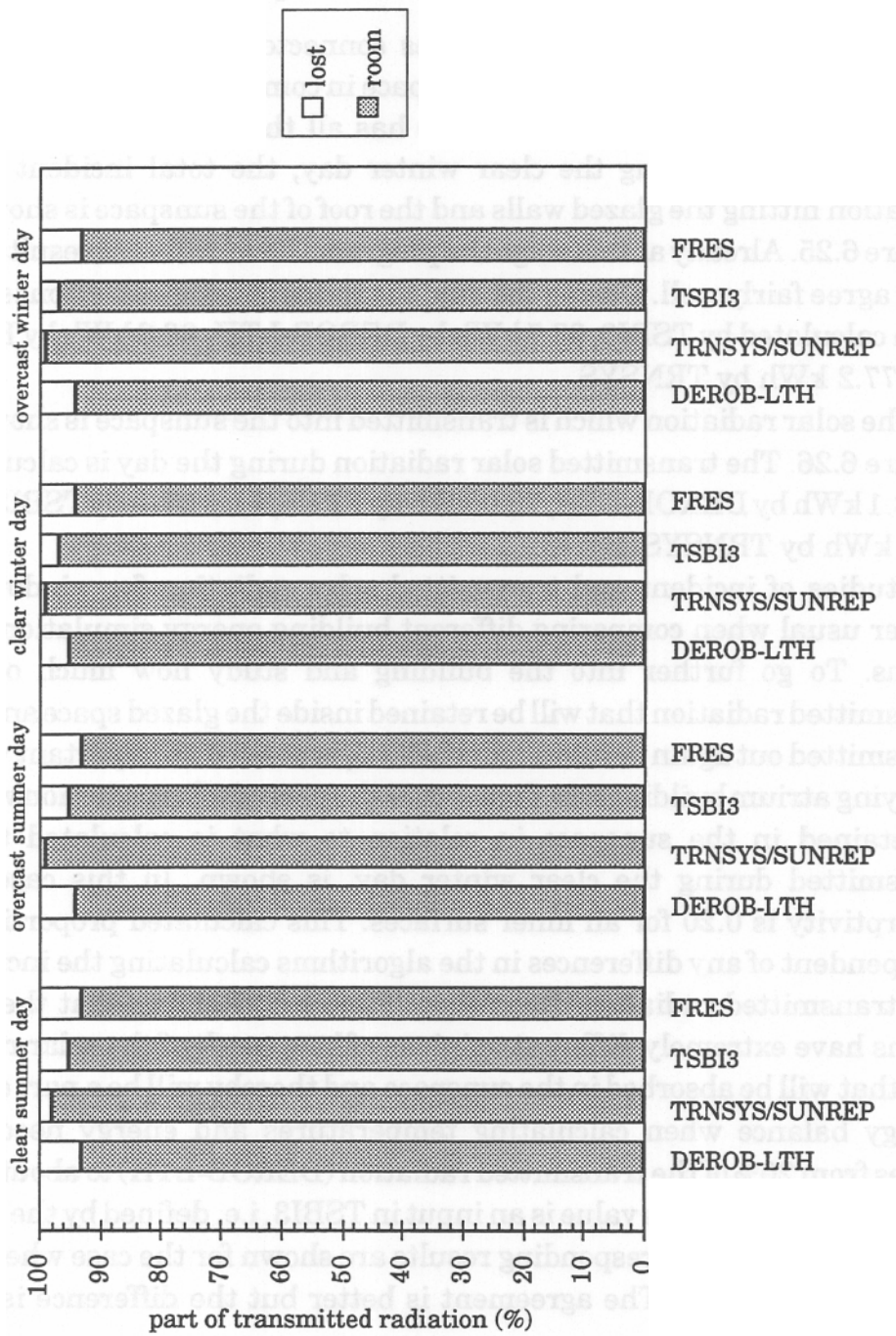


Figure 6.24 Solar energy balances for the shoebox.

the clear winter day is calculated to be 14.7 kWh by DEROB-LTH. By TRNSYS/SUNREP it is 21.9 kWh, by TSBI3 33.7 kWh and by FRES 42.4 kWh. With a higher absorptivity, 0.80, the result from TRNSYS/SUNREP is 29.8 kWh absorbed solar radiation, DEROB-LTH 32.7 kWh, TSBI3 42.3 kWh and FRES 46.2 kWh. The differences are smaller with a higher absorptivity. If everything would have been absorbed, the absorbed solar radiation would have been the same as the transmitted radiation.

The total solar energy balance, calculated for the clear winter day is shown in Figure 6.31. The transmitted solar radiation into the sunspace is defined as 100%. This is then divided into the part that is absorbed in the sunspace, the part that is absorbed in the room and the part that is lost to the outside by short wave radiation. The difference is very large between the programs as shown also in earlier figures.

The corresponding calculations for the clear summer day have also been made. In Figure 6.32 the calculated solar radiation hitting the outside of the sunspace with all surfaces glazed, is shown. It is almost impossible to see more than three curves, depending on that TRNSYS and DEROB-LTH have almost the same result. The total incident solar radiation during the day is calculated to 413 kWh by FRES, 387 kWh by TSBI3, 382 kWh by DEROB-LTH and 379 kWh by TRNSYS. In Figure 6.33 we can see that the difference is larger between the programs when calculating the transmitted radiation. The transmitted solar radiation is calculated to 354 kWh by FRES, 302 kWh by DEROB-LTH, 294 kWh by TSBI3 and 270 kWh by TRNSYS. Even if this should be acceptable, the difference between the calculated absorbed solar radiation in the sunspace is not, see Figure 6.34. This calculations are made for light surfaces, i.e. when the short wave absorptivity is 0.20. In Figure 6.35 the absorptivity is 0.80. In this case FRES and TSBI3 has similar results as well as TRNSYS/SUNREP and DEROB-LTH. Note that the percentage part of the transmitted solar radiation that will be absorbed in the sunspace and not lost to the outside, is input data in TSBI3. This means that the user has to make an assumption or use calculation results from other programs.

If the results are shown as absorbed solar energy during the summer day, it becomes obvious that the contribution from the sun is differing very much, see Figure 6.36 and 6.37. In Figure 6.36 the absorptivity is 0.20 and in this case the total solar radiation absorbed during the day is 63.9 kWh by DEROB-LTH, 102.2 kWh by TRNSYS/SUNREP, 176.4 kWh by TSBI3 and 267.5 kWh by FRES. With the absorptivity 0.80 the absorbed radiation is 145.3 kWh by TRNSYS/SUNREP, 165.5 kWh by DEROB-LTH, 213.3 kWh by TSBI3 and 291.6 kWh by FRES.

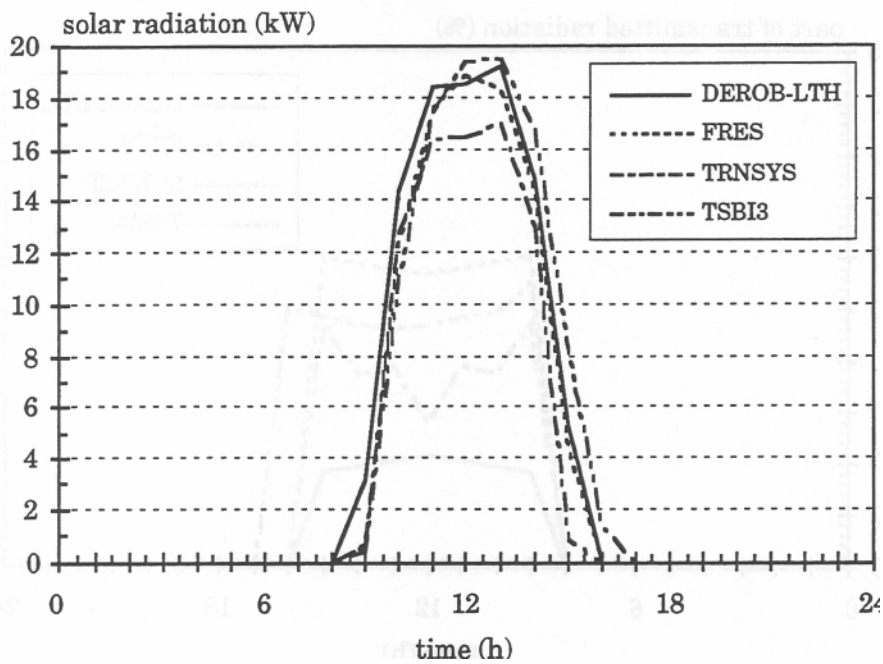


Figure 6.25 Incident solar radiation for the sunspace with all surfaces glazed during the clear winter day.

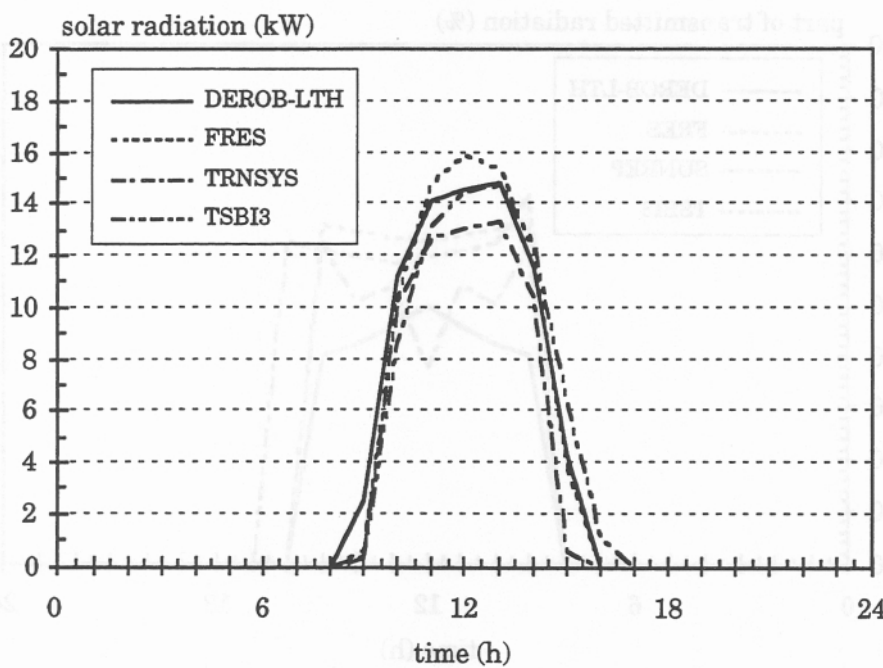


Figure 6.26 Solar radiation transmitted to the sunspace with all surfaces glazed during the clear winter day.

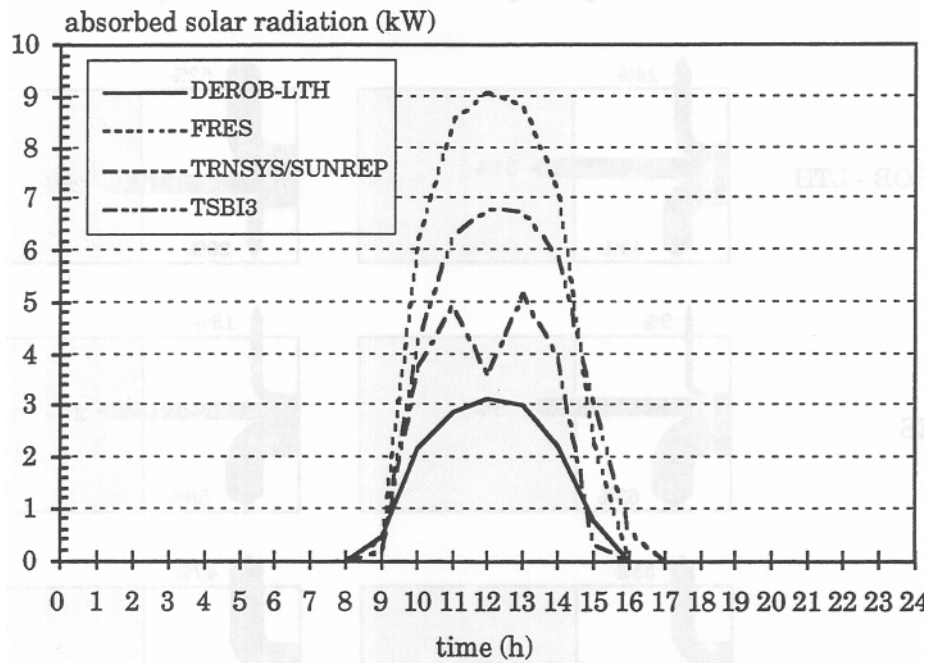


Figure 6.29 Absorbed solar radiation in the sunspace during the clear winter day. Absorptivity = 0.20.

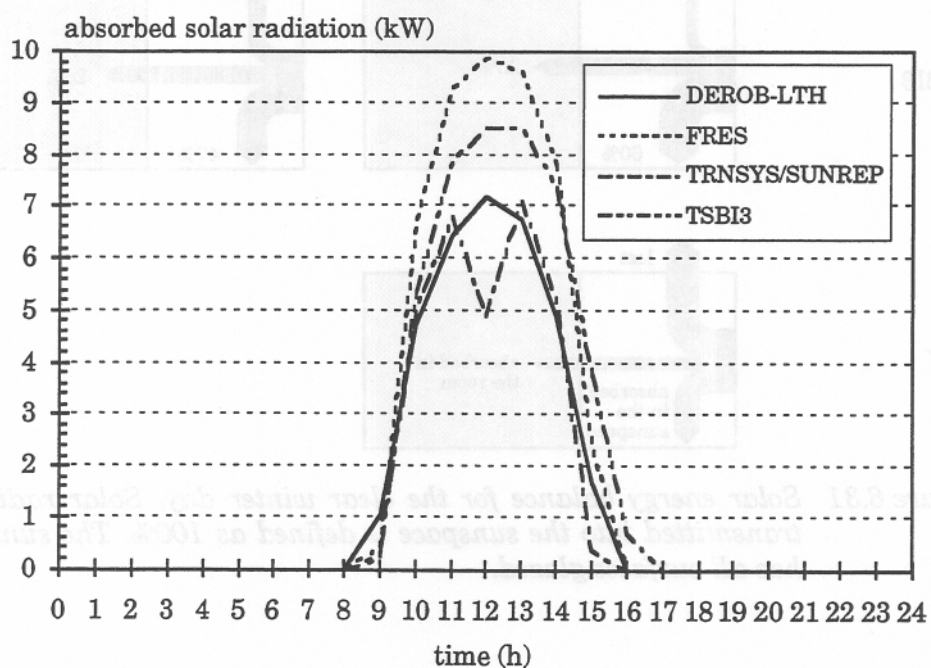


Figure 6.30 Absorbed solar radiation in the sunspace during the clear winter day. Absorptivity = 0.80.

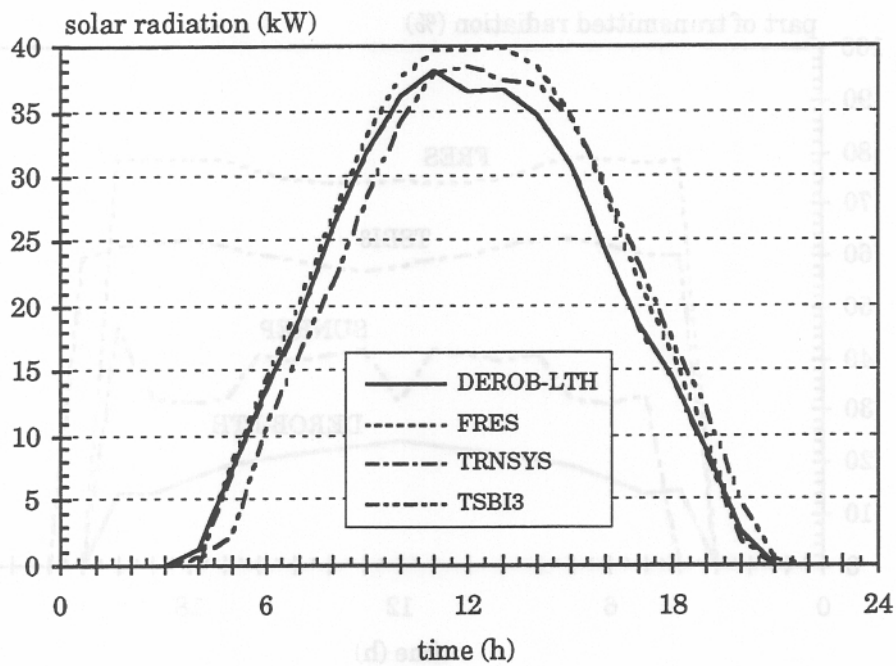


Figure 6.32 Incident solar radiation for the sunspace with all surfaces glazed during the clear summer day.

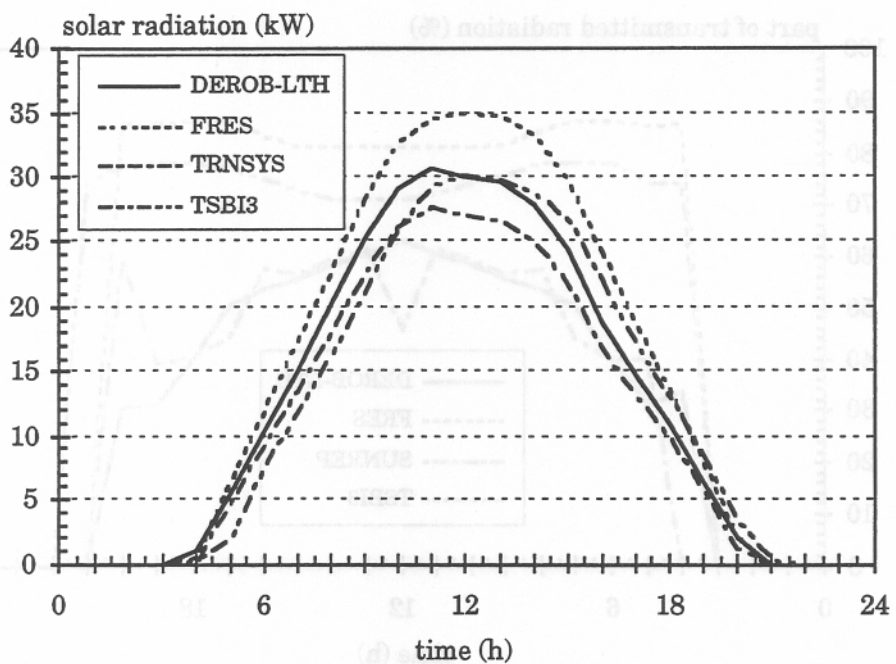


Figure 6.33 Solar radiation transmitted to the sunspace with all surfaces glazed during the clear summer day.

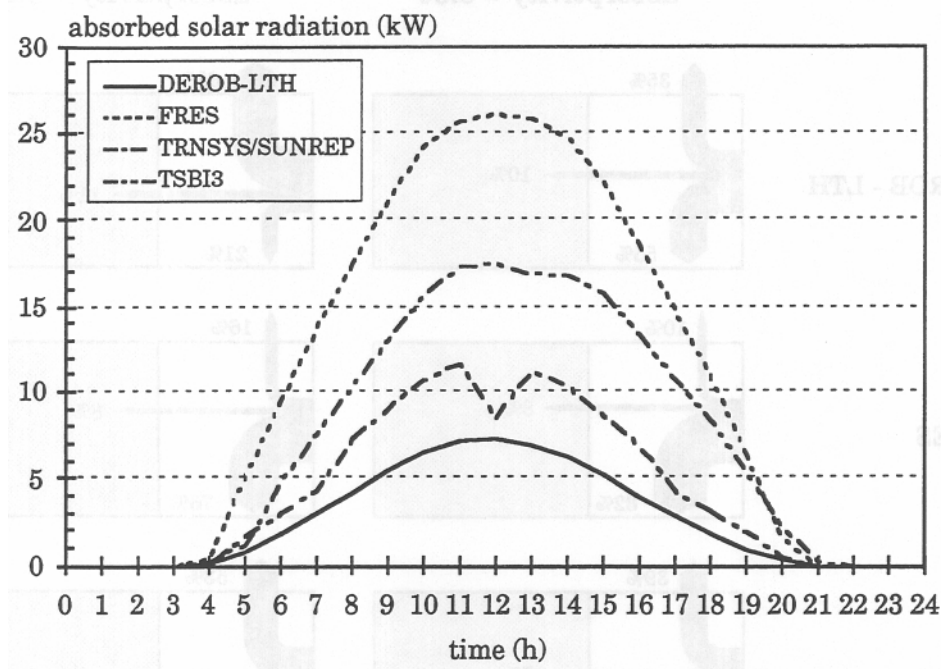


Figure 6.36 Absorbed solar radiation in the sunspace during the clear summer day. Absorptivity = 0.20.

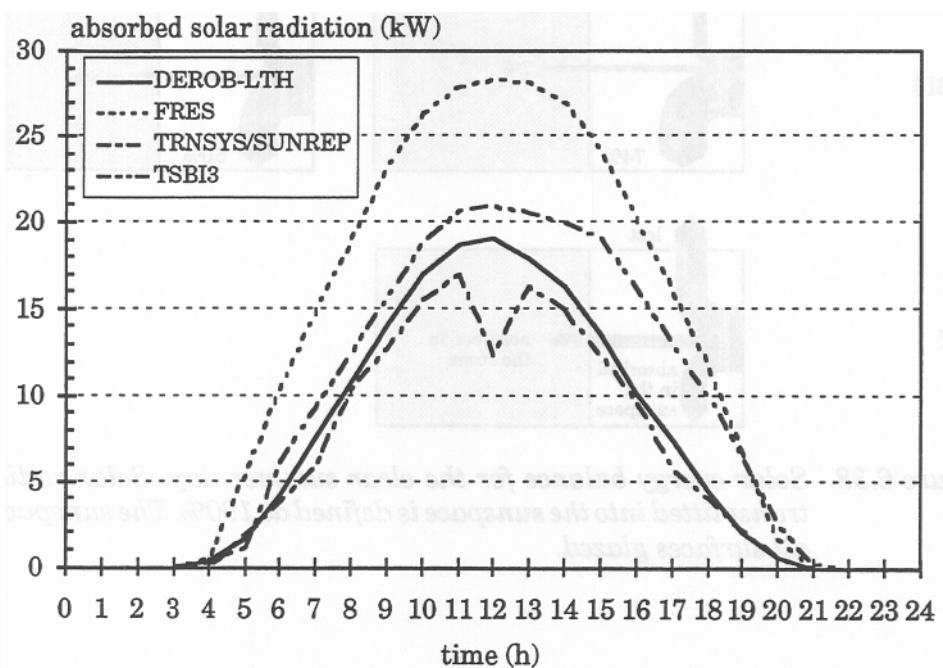


Figure 6.37 Absorbed solar radiation in the sunspace during the clear summer day. Absorptivity = 0.80.

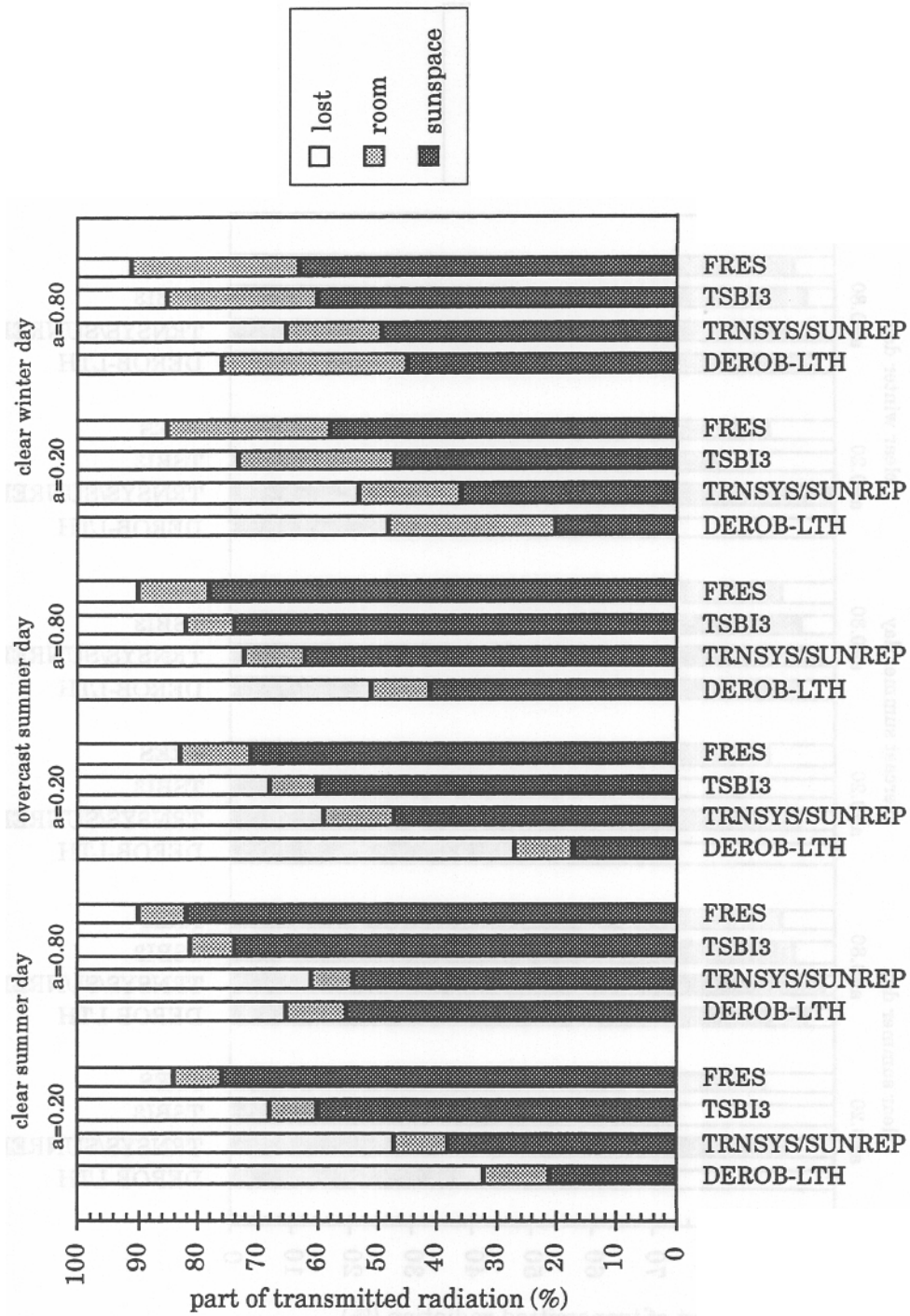


Figure 6.39 Solar energy balances for the shoebox combined with a sunspace with all surfaces glazed.

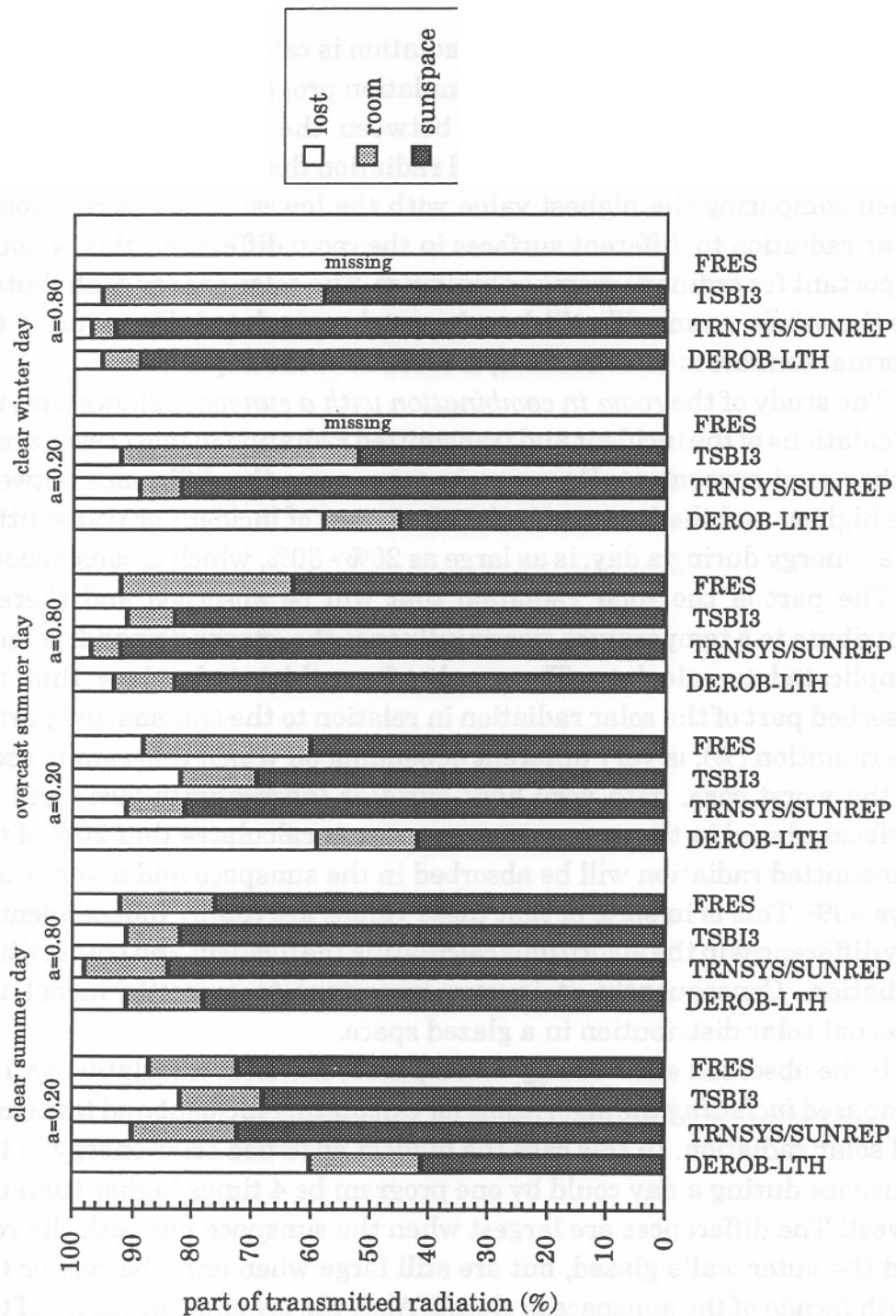


Figure 6.41 Solar energy balances for the shoebox combined with a sunspace with only the roof glazed.

In FRES, the transmitted solar radiation is absorbed in two steps. In the first step, the transmitted radiation is evenly absorbed only in the opaque surfaces, taken into account the absorptivity factor. The part that is not absorbed will be reflected. In the second step, the reflected radiation from step one will be evenly distributed to all surfaces. The opaque surfaces absorb all heat and the windows will absorb the part which is not transmitted. No further reflections will occur. This method is adequate for an ordinary room with relatively small windows (like the test room). The problem occurs when a large part of the room is surrounded by glazed surfaces, like a sunspace or an atrium. As the transmitted radiation in the first step only is distributed to opaque surfaces, the absorbed energy will be overestimated.

DEROB-LTH and SUNREP are using a geometrical description of the buildings in order to calculate which surfaces that will be hit by the sun and calculate absorption and reflections using view factors to distribute the solar radiation.

The results from DEROB-LTH and TRNSYS/SUNREP give in general significantly lower energy contribution from the sun than TSB13 and FRES. If atrium buildings or other types of glazed spaces are to be studied, it is essential to base the calculations on a geometrical description, taking into account transmission, reflections and absorptivity so that solar radiation can be transmitted out again directly or by reflection. Building energy simulation programs used for ordinary buildings are definitely not automatically suitable for atrium buildings.

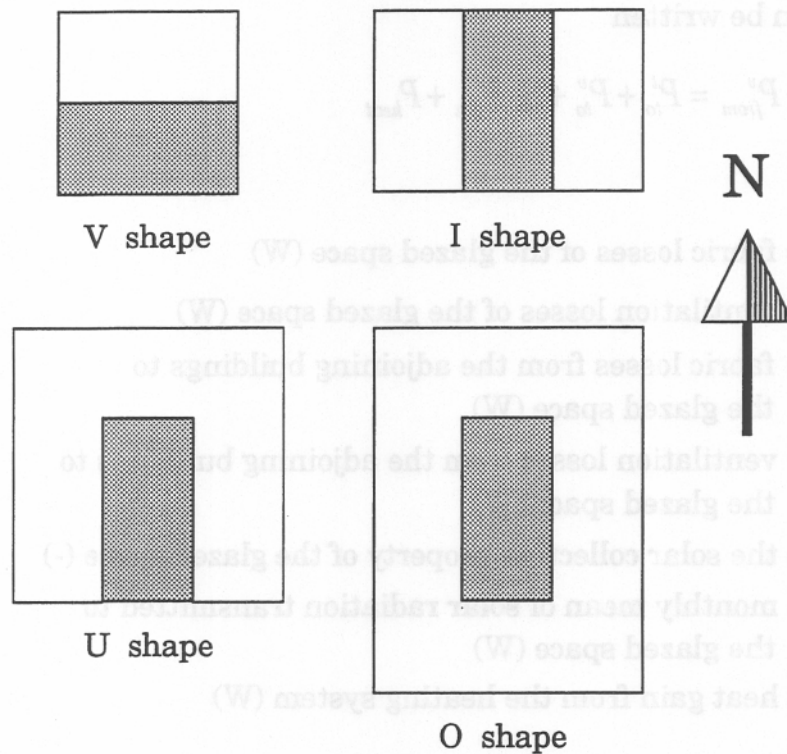


Figure 6.42 Plan and orientation of the studied glazed spaces.

Table 6.4 Properties of the glass types for perpendicular incidence.

Glass type	Trans- mission	Reflec- tion	Absorp- tion	U value (W/m ² °C)
single glass	0.85	0.08	0.07	5.88
double glass	0.72	0.13	0.15	2.94
triple glass	0.62	0.17	0.21	1.96

The study showed that the effect of the investigated factors can be ranked in the following order of significance. The ones at the top have the greatest significance, and those at the bottom the least.

- Absorptivity for short wave radiation of the inside surfaces of the glazed space (i.e. dark or light surfaces)
- The geometry of the space and the proportion of glazed surfaces
- The properties of the glazed construction
- Orientation
- Time of year
- Geographical position (latitude)

This means that the solar collection property S need not be calculated for different latitudes. It can also be considered constant over the year. On the other hand, the properties of the glazed space with regard to transmission of solar radiation cannot be ignored, nor can the geometry or the absorptivity of the inside surfaces.

The solar collection property S has therefore been calculated for the different types of glazed spaces for single, double and triple glazing. The value of S must also be calculated as a function of absorptivity. Obviously, there are many different variants of glazed space design, but all these cannot be predicted or shown here. The examples are intended to give an idea of the solar collection properties which different types of glazed spaces have, so that an approximative assessment of temperatures and energy requirement may be made.

6.11.3 Summary of solar collection property for variable absorptivity and geometry

The mean value of the solar collection property S over the year has been calculated for different values of absorptivity for the walls and floor which adjoin the glazed space. Climatic data from Lund, Sweden, for 1988 have been used (latitude 55.72°N , longitude 13.22°E), and the orientations are as shown in Figure 6.42. The results can however be used for other locations and for other orientations, see Wall (1994).

Values of the solar collection property S as a function of absorptivity are plotted for the four types of glazed space in Figure 6.43-6.46. The glazed spaces are described earlier in this chapter. Calculations have been made for single, double and triple glazing in the roof and glazed facades

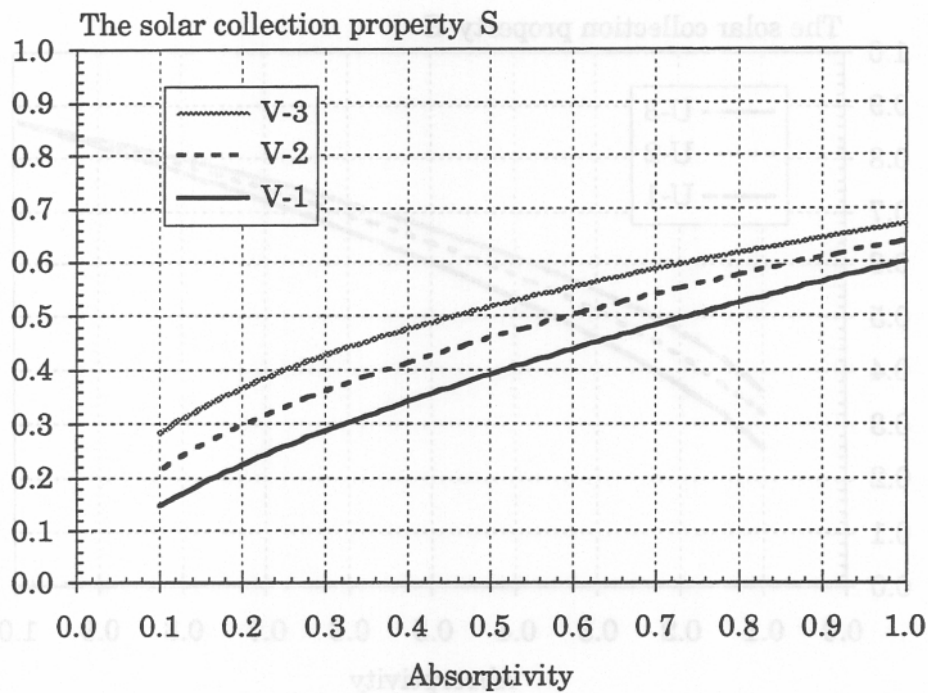


Figure 6.43 Solar collection property as a function of absorptivity for the glazed space with a building on one side.

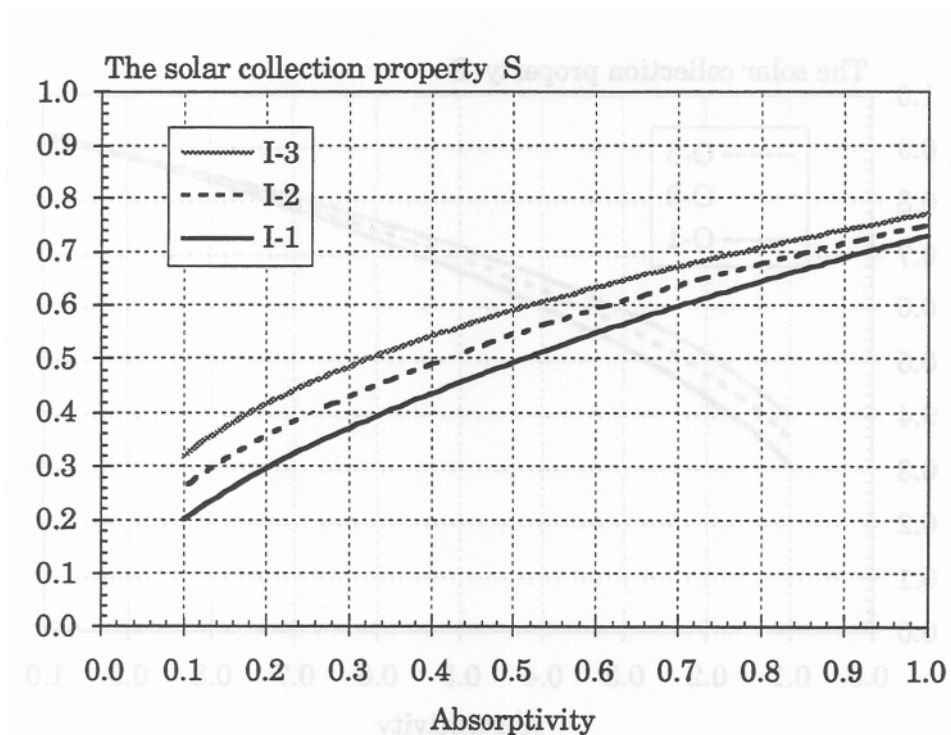


Figure 6.44 Solar collection property as a function of absorptivity for the glazed space with buildings on two sides.

6.11.4 The effect of inclined surfaces

To see how the solar collection property is influenced by the angle of the roof, calculations were also made with a 30° pitched roof. The results show that the solar collection property S is reduced with about 0.05-0.10 compared with a horizontal roof, when the glazed space has buildings on two, three or four sides.

The calculation error of the utilised solar radiation will be minimized if the above calculated values of S is used in combination with transmitted solar radiation for a simplified horizontal roof. With this simplified geometry, the calculation error of the utilised solar energy will be less than 1% with single glazing. With triple glazing, the error will be about 3-4%.

The solar collection property S for the glazed space with a building on only one side, will increase with about 0.05 when the roof has an angle of 30° or the glazed wall an angle of 60° instead of a horizontal roof or vertical walls. In this case the transmitted solar radiation should be calculated for the actual angle of the surfaces. In combination with the above calculated values of S , the utilised solar radiation will be underestimated with about 10%. In order to reduce this error further, add 0.05 to the chosen value of S in Figure 6.43, then the error will be minimal.

evaluated. The method is based on calculations with DEROB-LTH, which is a building energy simulation program using a geometrical description of the buildings to calculate the solar radiation.

An example of a method calculating shadows is also presented. The method has been implemented in a PC software application, called Xsun, which can function as a stand-alone design tool or maybe integrated with programs for thermal simulation of buildings or solar systems. An example is given where Xsun is integrated with the thermal simulation tool TSBI3.

H	time (civil time) (h)
H_{τ}	the current half hour (h)
H_{ts}	the true solar time (h)
h_c	surface heat transfer coefficient ($\text{W/m}^2\text{C}$)
$h_k, k=0$	total outside film coefficient ($\text{W/m}^2\text{K}$)
$h_k, k>0$	total conductivity between the pane k and $k+1$ ($\text{W/m}^2\text{K}$)
I	short wave radiation (W/m^2)
I_i	incident radiation (W/m^2)
I_{fi}	forward incident radiation (W/m^2)
I_a	absorbed radiation (W/m^2)
I_{fa}	absorbed part of forward incident radiation (W/m^2)
I_{fj}	forward directed radiation in front of layer j (W/m^2)
I_{fr}	reflected part of forward incident radiation (W/m^2)
I_{ft}	transmitted forward directed radiation (W/m^2)
I_{Ag}	reflected radiation from the surface of the ground (W/m^2)
$I_{Ag,\theta i}$	reflected radiation from the surface of the ground, angle of incidence (W/m^2)
$I_{Ag,\theta t}$	reflected radiation from the surface of the ground, sloped surface (W/m^2)
I_{ba}	absorbed part of backward incident radiation (W/m^2)
I_{bi}	backward incident radiation (W/m^2)
I_{bj}	backward directed radiation in front of layer j (W/m^2)
I_{br}	reflected part of backward incident radiation (W/m^2)
I_D	insolation of direct solar radiation (W/m^2)
I_{Dt}	transmitted direct solar radiation (W/m^2)
I_{dt}	transmitted diffuse solar radiation (W/m^2)
I_{dDt}	transmitted diffuse and direct solar radiation (W/m^2)
I_{d1}	incident diffuse solar radiation (W/m^2)
I_{d2}	total reflected solar radiation from the ground (W/m^2)
$I_{d,\theta i}$	diffuse solar radiation on a sloping surface (W/m^2)
I_{dV}	diffuse solar radiation on a vertical surface (W/m^2)
I_{di}	total incident diffuse solar radiation on the surface (W/m^2)
I_{Di}	total incident direct solar radiation on the surface (W/m^2)
$I_{Di,c}$	total incident direct solar radiation on the surface with an amount of cloud N_c (W/m^2)
$I_{D,\theta i}$	direct solar radiation on a sloping surface (W/m^2)
$I_{D\theta,C}$	direct solar radiation on an arbitrary surface (W/m^2)
$I_{dB,c}$	diffuse background radiation (W/m^2)
I_H	global solar radiation (W/m^2)
$I_{H,c}$	global solar radiation, cloudy sky (W/m^2)
I_{dH}	horizontal diffuse solar radiation (W/m^2)
$I_{dH,c}$	horizontal diffuse solar radiation, cloudy sky (W/m^2)
I_{DH}	horizontal direct solar radiation (W/m^2)
$I_{DH,c}$	horizontal direct solar radiation, cloudy sky (W/m^2)
I_{DN}	direct solar radiation, normal incidence (W/m^2)
$I_{DN,C}$	direct solar radiation at normal incidence, cloudy sky (W/m^2)
I'_{DN}	direct solar radiation, normal incidence, dry atmosphere (W/m^2)
I_o	the solar constant (W/m^2)

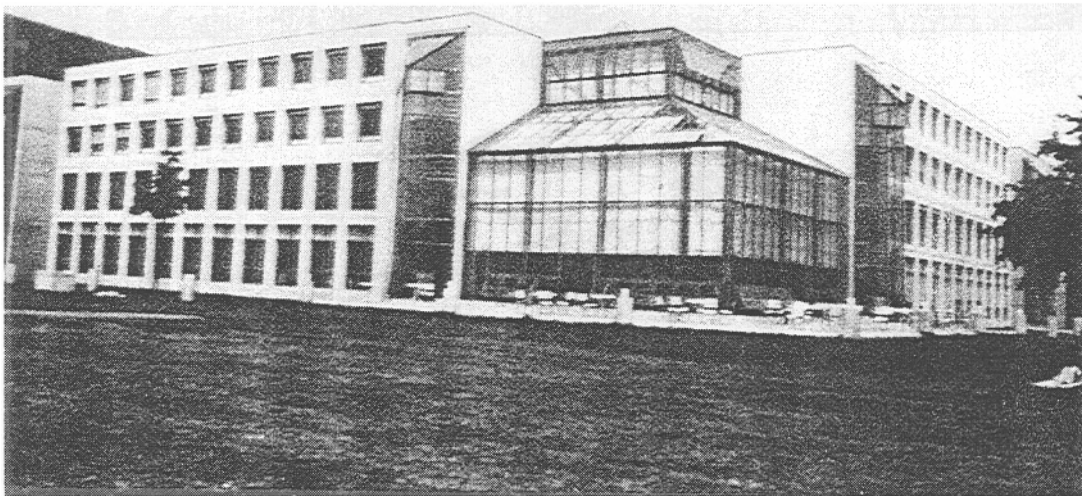
P_{tot}	total incoming short wave radiation to the windows (W)
$P_{tot,gl}$	total incoming short wave radiation to the outside of the glazings of the sunspace (W)
P_{trans}	total short wave radiation transmitted to the room (W)
$P_{trans,gl}$	total short wave radiation transmitted to the sunspace (W)
P_{eci}	the radiation received by surface i (W)
P_{ceil}	resulting short wave radiation to the ceiling, part of P_{trans} (%)
P_{east}	resulting short wave radiation to the east wall, part of P_{trans} (%)
P_{floor}	resulting short wave radiation to the floor, part of P_{trans} (%)
P_{north}	resulting short wave radiation to the north wall, part of P_{trans} (%)
P_{south}	resulting short wave radiation to the south wall, except for windows, part of P_{trans} (%)
P_{west}	resulting short wave radiation to the west wall, part of P_{trans} (%)
P_{win}	resulting short wave radiation to the windows (inside), part of P_{trans} (%)
P_{net}	the part of P_{trans} that stays in the room (W)
$P_{net,gl}$	the part of $P_{trans,gl}$ that stays in the sunspace (%)
P_{to}^t	fabric losses from the adjoining buildings to the glazed space (W)
P_{from}^t	fabric losses of the glazed space (W)
P_{to}^v	ventilation losses from the adjoining building to the glazed space (W)
P_{from}^v	ventilation losses of the glazed space (W)
P_{heat}	heat gain from the heating system (W)
P_{sun}	monthly mean of solar radiation transmitted to the glazed space (W)
\hat{p}_1	position of the sun in a coordinate system (-)
\hat{p}_2	position of the sun in a cardinal coordinate system (-)
q	energy flux at a surface (W/m^2)
R	long wave radiation (W/m^2)
R_A	atmospheric long wave radiation (W/m^2)
$R_{A,c}$	atmospheric radiation when the sky is completely covered by cloud (W/m^2)
R_{A,N_c}	long wave radiation from the atmosphere for an amount N_c of cloud (W/m^2)
R_G	long wave radiation from the ground (W/m^2)
R_{G,N_c}	long wave radiation from the ground at broken cloud cover (W/m^2)
R_{Geff}	effective thermal radiation from the ground, clear sky (W/m^2)
$R_{Geff,c}$	effective thermal radiation from the ground, cloudy sky (W/m^2)
R_s	radiation from a black surface (W/m^2)
R_d	a ratio for calculation of incident solar radiation (Eq. 6.119) (-)
R_g	a ratio for calculation of incident solar radiation (Eq. 6.120) (-)
r	reflectance (-)
r_1	reflectance, 1st media (-)
r_2	reflectance, 2nd media (-)
r_3	reflectance, 3rd media (-)
r_b	reflection of backward directed radiation (-)
$r_{b,j}$	reflection of backward directed radiation at layer j (-)
r_c	the reflectance at normal incident for the window (-)
r_f	reflection of forward directed radiation (-)

α_d	coefficient of absorption for particulate scatter (-)
α_r	coefficient of absorption for molecular scatter (-)
β	coefficient of turbidity
ε_g	long wave emissivity of ground (-)
ε_r	long wave emissivity of surface (-)
Φ_H	$2\pi (t-6) / 24$ (rad)
Φ_l	$(90^\circ - \text{latitude}) \cdot \pi / 180$ (rad)
γ	electric permittivity (As/Vm)
η	coefficient used for calculation of diffuse solar radiation (Eq. 6.21)
κ	constant between 0.30 and 0.35 (Eq. 6.19) (-)
λ	wavelength (μm)
μ	magnetic permeability (Vs/Am)
$\theta_1, \theta_2, \theta_3$	plane angles (rad)
θ_α	the solar azimuth angle ($^\circ$)
θ_β	the horizontal angle between the normal and the direction of radiation ($^\circ$)
θ_d	declination of the sun ($^\circ$)
θ_γ	the angle between the normal to the surface and the horizontal plane ($^\circ$)
θ_g	longitude of the locality ($^\circ$)
θ_l	latitude of the locality ($^\circ$)
θ_H	hour angle ($^\circ$)
θ_h	the solar height angle (rad)
$\theta_{h,opt}$	the optical solar height (rad)
θ_i	the angle of incidence ($^\circ$)
θ_r	angle of reflection ($^\circ$)
θ_s	sunrise hour angle ($^\circ$)
θ_t	inclination of surface to the horizontal plane ($^\circ$)
θ_{ts}	the true solar time (rad)
θ_v	south azimuth of the surface ($^\circ$)
θ_w	the orientation of the surface ($^\circ$)
θ_z	zenith angle ($^\circ$)
σ	Stefan-Boltzmann constant, $(5.70 \cdot 10^{-8} \text{ W/m}^2\text{K}^4)$
v_1	solar angle with the south ($^\circ$)
v_2	solar angle with the east ($^\circ$)
w	quantity of water which can be precipitated (kg/m^2)
w_N	$2\pi / 366$ (rad)

- Källblad, K. (1973). *Strålning genom glaskombinationer, Principer och datorprogram* (In Swedish) (Report 1973:12). Lund (Sweden): Department of Building Science, Lund Institute of Technology.
- Liljequist, G. H. (1979). *Strålning* . (*Radiation*). (In Swedish). Uppsala (Sweden): University of Uppsala, Department of Meteorology.
- Lund, H. (1977). *SOLIND - Program til beregning af solindfald*, (SOLIND - Program for calculation of solar irradiation) (In Danish). Lyngby: DTH, Thermal Insulation Laboratory.
- Petersen, E. (1982). *Solstråling og dagslys, - målt og beregnet*. (Solar Radiation, - Measured and Calculated) (In Danish) (Report 34). Lyngby: Lysteknisk Laboratorium.
- Rogers, D. F. (1985). *Procedural Elements for Computer Graphics*, pp. 179-185, McGraw-Hill Book Company.
- Seller, W. D. (1965). *Physical climatology*. University of Chicago Press, Chicago & London.
- Stephenson, D.G. (1965). Equations for Solar Heat Gain through Windows. *Solar Energy*, Vol 9 Nr 2 april-june 1965.
- Taesler, R. & Andersson, C. (1985). *En metod for beräkning av solstrålning från normala meteorologiska observationer. (A method for the calculation of solar radiation from normal meteorological observations)*. (In Swedish) (SEAS Sheet No 1). Stockholm (Sweden): Royal Institute of Technology, Department of Heating and Ventilation.
- Taesler, R. (1972). *Klimatdata för Sverige (Climatic data for Sweden)*. (In Swedish). Stockholm (Sweden). Swedish Council for Building Research.
- Taesler, R. (1985). *Klimatberoendet i bebyggelsens energibudget. Data och beräkningsmetoder (The dependence of the energy budget of buildings on climate. Data and calculation methods)*. (In Swedish) (Report No R116:1985). Stockholm (Sweden): Swedish Council for Building Research.
- Thekaekara, M. P. (1973). *Solar Energy*, 14, 107-27. Pergamon.
- Wall, M. (1994). *Projekteringshjälpmedel för inglasade rum. Klimat och energi. (A design tool for glazed spaces. Climate and energy)*. (In Swedish). Lund (Sweden): University of Lund - Lund Institute of Technology, Department of Building Science.

7. Test studies

7.1 Neuchâtel University - NUNI



Building type	Education
Passive solar features	Direct daylighting Sunspace
Occupancy date	October 1986
Floor area	8.100 m ²
Annual delivered fuel	Heating energy 215 MJ/m ² (estimated)
Architects	NCL Architecture-urbanisme
Energy consultant	Sorane SA
Client	Canton de Neuchatel

7.1.1 Summary

The new building of the faculty of literature of the University of Neuchatel has a heating energy demand of only 215 MJ/m²,an. The symmetrical building has a central courtyard and attached sunspace. It is heated by a heatpump with backup on extremely cold days from district heating. The prominent large sunspace was conceived as a passive solar heated space. The building is deliberately not air conditioned and only special rooms have mechanical ventilation. The glazed space is tempered in summer through natural ventilation and evaporative cooling from pools of water.

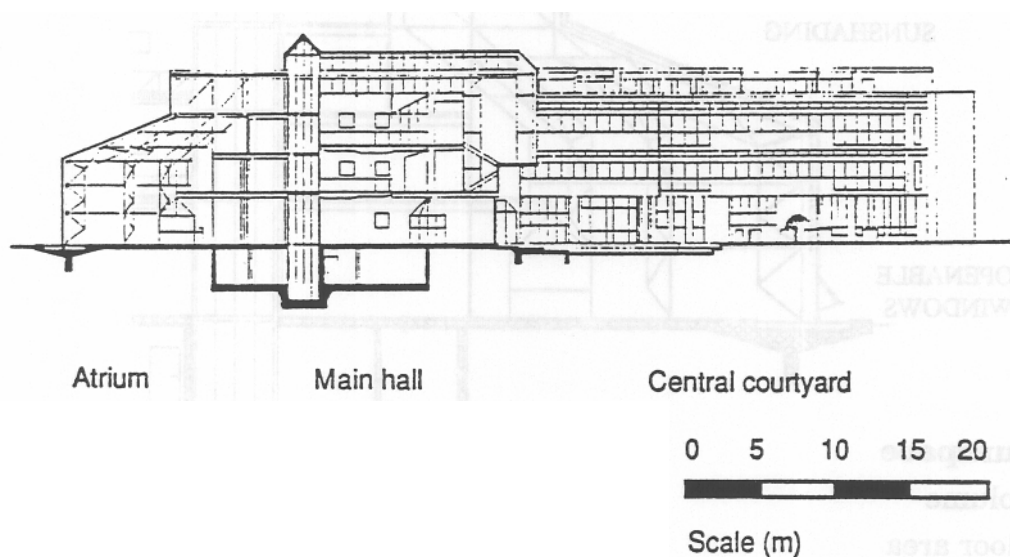
7.1.3 Building form

The 3-4 story building complex, organized around a central court, is comprised of six blocs :

- Four nearly identical blocks housing a library, class rooms and offices
- A 12 x 12 x 12 m sunspace with 160 m² of vertical glass and 130 m² of sloping glass
- A central block with the entry hall, cafeteria and commons area

A pedestrian axis passing diagonally through the building connects the town to the open park land foreseen for festivals. This axis passes through the commons area which can be used independently from the normal operations of the building.

Volume	Gross 24'600 m ³
Floor area	Gross 8'100 m ²
Number of levels	4 + basement



7.1.4 Building construction

The concrete framing, ductwork and other services are all exposed rather than hidden with a suspended ceiling. the construction is based on a 7.2 m grid. The sunspace is single glazed to the outside and to the building side.

U-Values (W/m ² K)	
Windows	3.10 and 1.60
Walls	0.35
Building	0.70

7.1.7 Costs

The entire building complex was estimated to cost Sfr. 17,500,000. Actual costs were 20 percent higher. Part of this overcost included additional insulation, decided upon during the course of construction.

7.1.8 Energy performance

The estimated annual energy consumption for heating is 215 MJ/m²,a.

7.1.9 Human factors

The frequent and full occupancy of the sunspace proves its success as a gathering space. Students are apparently willing to accept cooler temperatures of the space in the winter in order to enjoy the amenity of the "outdoor" character of the space.



7.1.10 Energy saving achieved by the atrium

In winter the atrium is not heated, it is used as a buffer zone. In this way the amount of energy saved has been evaluated to 28 MWh/year.

This correspond to 4 % of the annual energy consumption of the whole university building (654 MWh/an).

7.1.12 Typical internal air temperature profiles

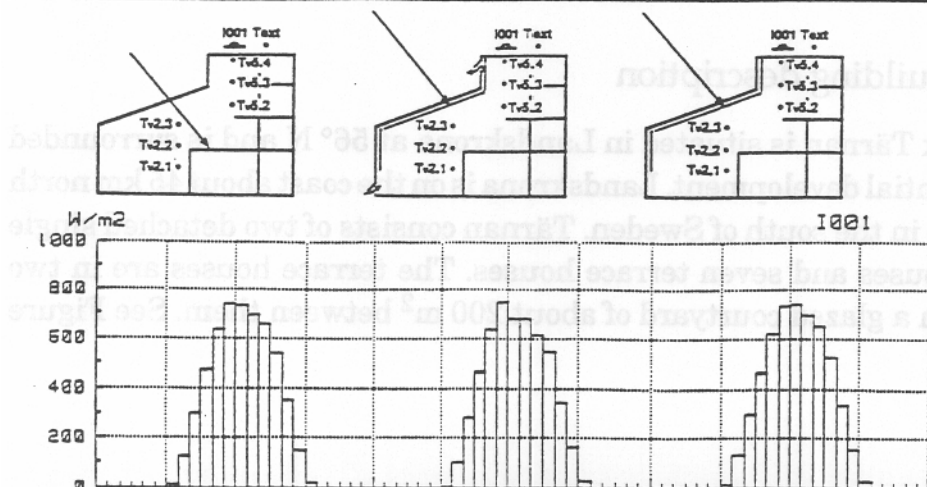
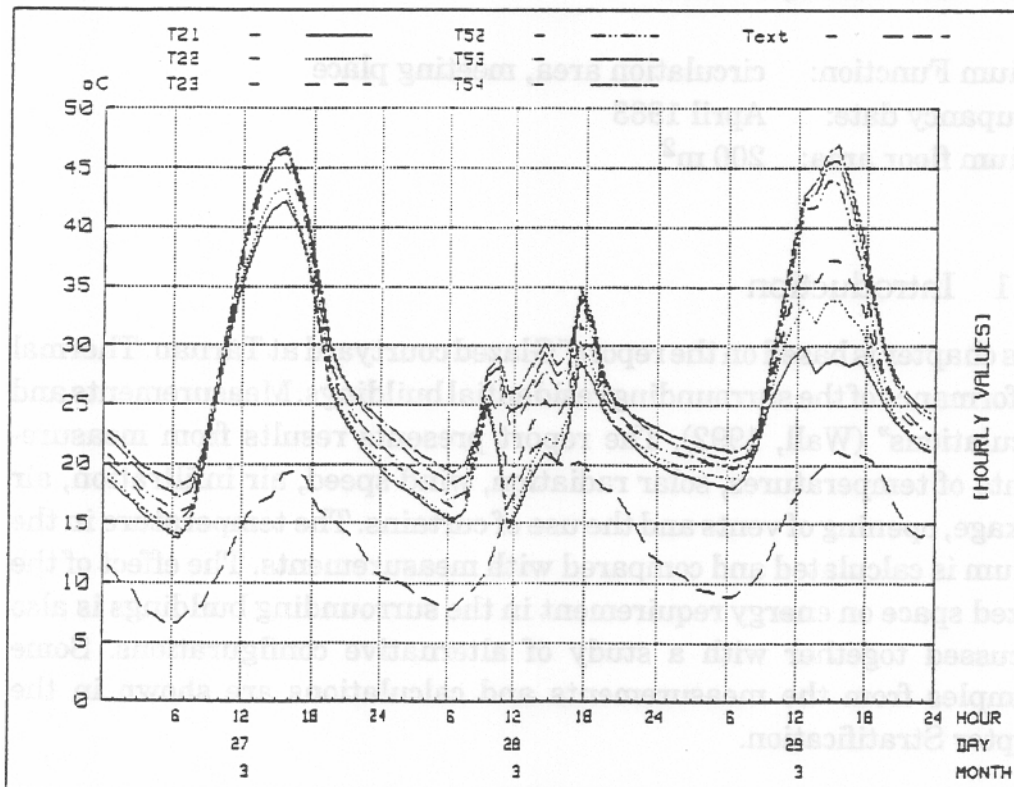
In the next figure three typical sunny days are presented.

During the **first day** no internal shading as well as no natural ventilation (opened hatches) are used.

The air temperature is not very stratified (only 4 degrees).

During the **third day**, the hatches are closed but the internal shading devices are used, in this way if the peak temperature in the upper part of the atrium has not changed in comparison to the first day, the lower part is 15K under the peak temperature !

Finally during the **second day** the internal shading devices are used and the hatches opened (from 10.30 a.m.). In this way, the stratification is reduced (8-10°C) and the temperature in the occupied zones becomes comfortable.



7.2.1 and 7.2.2. Together, they form a tenant-owner association. The terrace houses are on 2.5 storeys with a floor space of 123 m² and contain 5 rooms plus kitchen. In the vicinity of the dwellings there is a communal refuse storage room/store and a building housing the heat pumps.

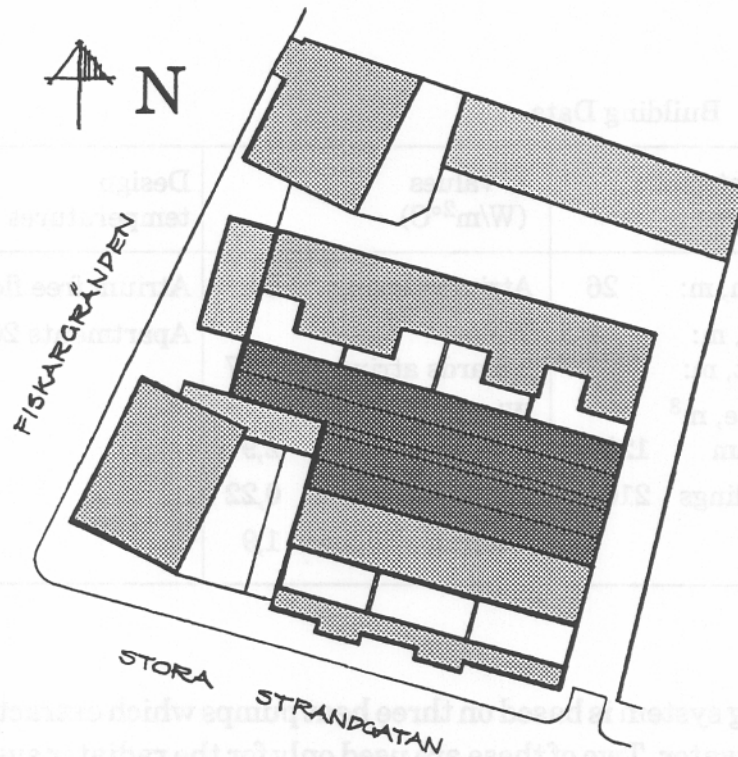


Figure 7.2.2 Layout plan, Tärnan.

The loadbearing walls of the buildings consist of prefabricated concrete units with cast-in timber studs. Between the studs the wall units contain mineral wool which is covered by a plastics foil and gypsum plasterboard.

The facades towards the external air consist mainly of painted concrete units with internal mineral wool insulation and gypsum plasterboard. Towards the courtyard the walls are clad with minerite fibre cement slabs, with mineral wool and gypsum plasterboard on the inside. The U value of the walls towards the courtyard is 0.27 W/m²°C (145 mm mineral wool) and the windows are reduced to double glazing. Towards the external air the windows are triple glazed, and the walls towards the external air, which have extra insulation, have a U value of 0.22 W/m²°C (45+145 mm mineral wool).

The floors consist of prefabricated concrete units with cast-in studs, with the concrete on the bottom. The ground floor slab has 195 mm mineral wool, and the intermediate floor 50 mm.

Vents are provided in both the roof and the gables. About 25% of the roof surface can be opened. In the roof there are horizontal curtains of acrylic fabric which are used both as insulation and for solar control.

The vents and curtains are controlled automatically by means of a special control equipment made by Dansk Gartneri Teknik (DGT) Sweden AB. This system has long been used in greenhouses. The control equipment is connected to temperature sensors and a smoke detector in the courtyard, and to humidity (rain), light and wind sensors outside.

When the temperature in the courtyard reaches a certain preset value, the vents are opened. If it begins to rain, the vents are half shut, and if there is strong wind, they are shut so that they have 10% opening area. The vents on the leeward side are opened first. These vents are opened to a larger angle than those on the windward side. The side which is to the leeward is determined by measurement, but it can also be set on the controls manually.

When the temperature in the courtyard reaches a certain (high) level, the curtains are drawn across in one layer, see Figure 7.2.3. A gap is left in the middle so that warm air can easily rise and leave through the open vents. The curtains are also controlled by a light meter.

At night when it is dark and cold, the curtains are drawn across in two layers to provide insulation, see Figure 7.2.3. The curtains can also be used as insulation in daytime when it is very cold outside. If the curtains were drawn during the night, they are opened in stages in the morning so that the cold downdraught should not be too strong for the plants. On the whole, the control of the vents and curtains can to a large extent be tailor-made for each project.

In principle, the courtyard is unheated. However, in order that the plants should survive, two 9 kW building driers have been used to prevent the temperature dropping below freezing.

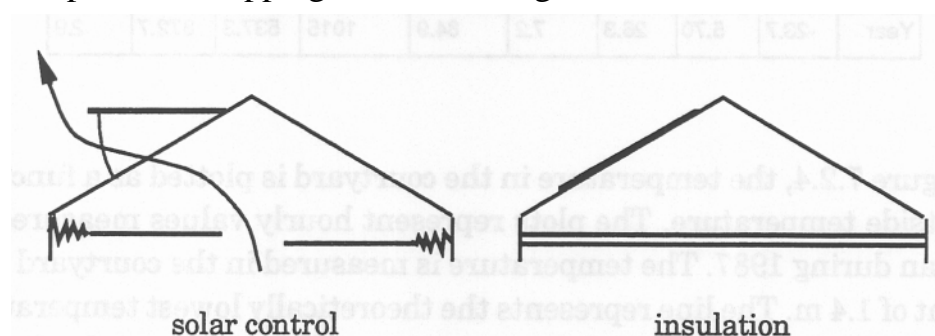


Figure 7.2.3 Use of the curtains as solar control and as insulation.

measurements deviate from the line. The reason for this is that two 9 kW building driers have been placed in the courtyard in order to maintain the temperature above freezing so that the plants can survive.

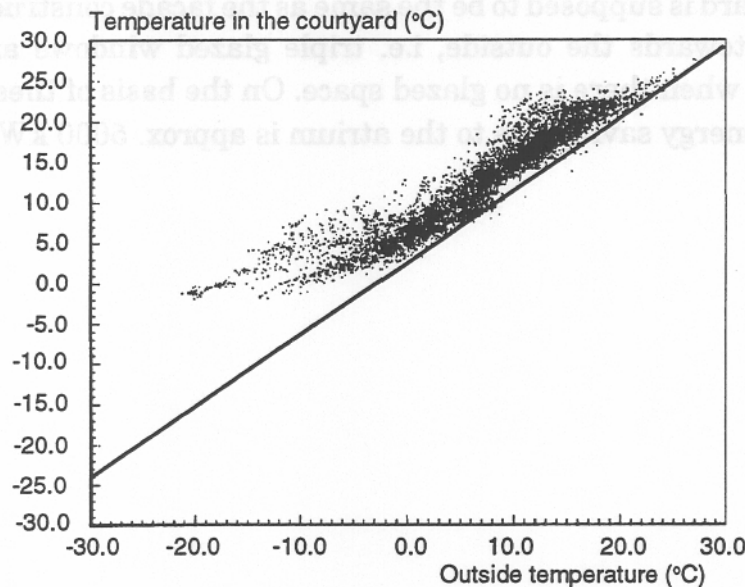


Figure 7.2.4 Temperature in the courtyard measured at a height of 1.4 m during 1987 as a function of outside temperature. The plots represent measured hourly values. The line represents the calculated lowest temperature in the courtyard under passive climatic control conditions, without solar radiation.

The air change rate in the atrium with the vents closed was measured as approx. 0.6 ach. On this occasion, in May, the outside temperature was 20°C and the temperature in the atrium was approx. 25°C. The wind speed was 2 m/s and the global solar radiation was 700–800 W/m². A fan pressurization test showed that at an overpressure at 50 Pa inside the atrium, the leakage flow was equal to 8.8 ach. See section Natural Ventilation and Infiltration.

The effect of the glazed courtyard on energy requirement in the surrounding buildings can be calculated as a reduction of the fabric and ventilation losses from the buildings surrounding the glazed courtyard. Since, generally speaking, the temperature in the courtyard during the heating season is higher than the outside temperature, the fabric losses from the surfaces abutting onto the courtyard decrease. In addition, the supply air temperature is higher in the 7 terrace houses which take their supply air from the courtyard.

From October to April, the temperature in the glazed courtyard is, on average, about 3–5°C higher than the outside temperature when the glazed space is not heated. The temperature difference varies depending on climatic variations in different years.

7.3 Bertolt Brecht Secondary School, Dresden



Atrium function:	Students' common and reading room
Completion of school building:	1970
Completion of atrium:	March 1994
Completion of school building's Energetic retrofitting	Autumn 1995
Heating energy demand of School building:	212 kWh/m ² a (before retrofit) 63 kWh/m ² a (after retrofit)
Heating energy demand of atrium:	not heated

7.3.1 Introduction

In the sixties and seventies, many schools in East Germany were built with open courtyards. These buildings have a very high heating energy demand and also have become too small. The Bertolt Brecht Secondary School in Dresden is an example for all school buildings of this type. It was studied with regard to an appropriate energetic building retrofit. To gain additional usable floor areas and to save heating energy, the courtyards have been roofed over with glass.

average U-value was about $2.1 \text{ W/m}^2\text{K}$, after retrofitting it is about $0.57 \text{ W/m}^2\text{K}$.

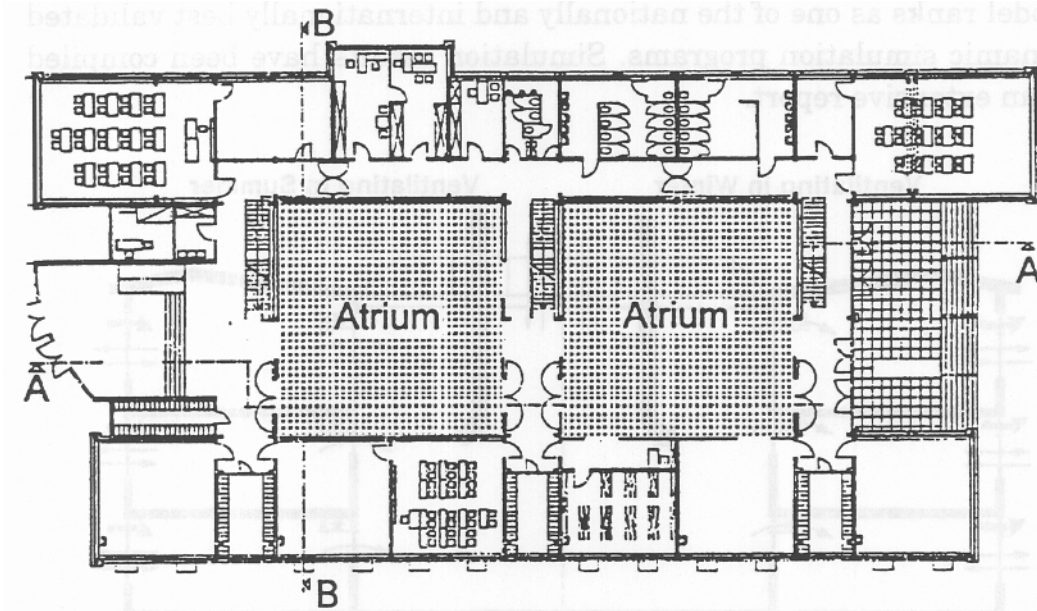


Figure 7.3.1: Ground Level Plan, Bertolt Brecht School

Table 7.3.2: Building Data

Characteristic Dimensions of one Atrium (West)	U-Values [$\text{W/m}^2\text{K}$]	Design Temperatures
length [m] 14.5	- atrium glazing: 1.3	- atrium: not heated
width [m] 14.5	- windows in exterior walls: 1.3	- school: 20°C
height [m] 11	- wall towards atrium: 1.8	
volume [m^3] 2300		

The remaining air change of $2510 \text{ m}^3\text{h}^{-1}$ is supplied directly by the outdoor air. For the other heated, non-classroom spaces of the school building with a volume of 8830 m^3 , a ventilation through the atrium is not planned. The air change assumed for calculation amounts to 0.5 h^{-1} .

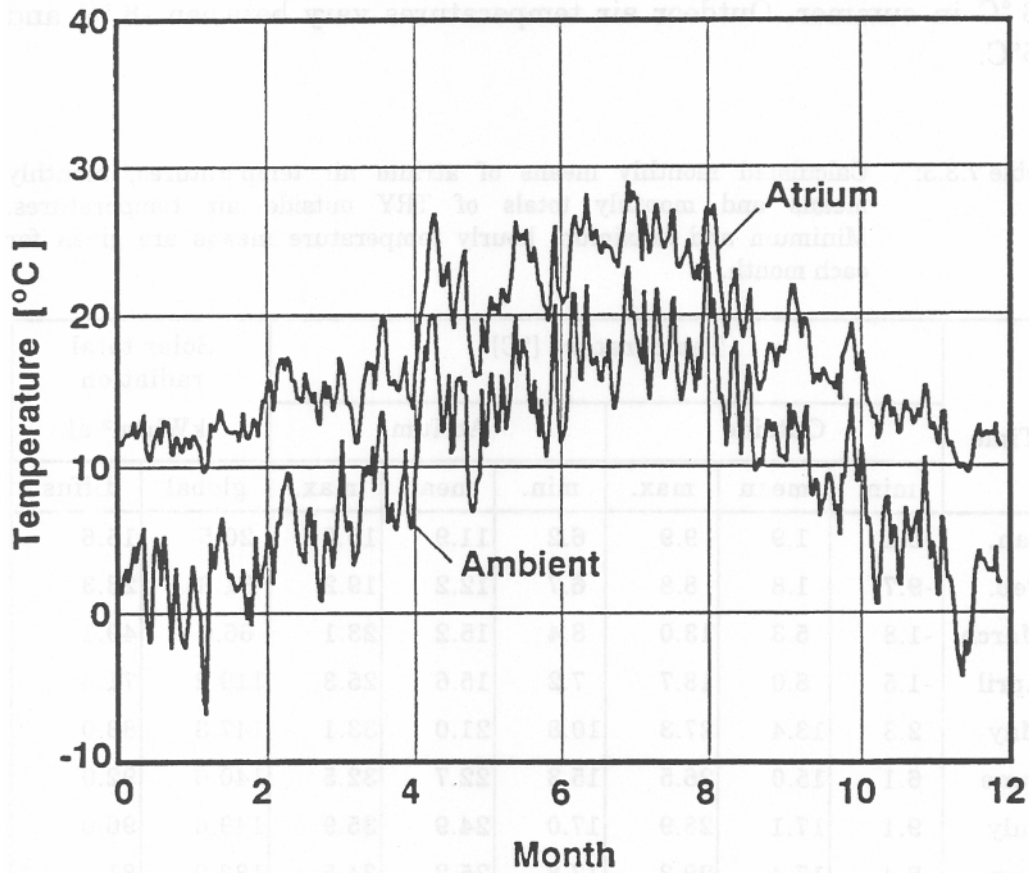


Figure 7.3.3: Calculated daily means of atrium air temperatures and daily means of TRY outside air temperatures.

The air change between atrium and ambience is assumed to come to 0.5 h^{-1} which is corresponding to an air change of $2300 \text{ m}^3\text{h}^{-1}$. In the summer months (May-September) the direction of air supply is reversed. As far as the calculated air temperatures in the atrium, it is assumed that an average outdoor air current of $8800 \text{ m}^3\text{h}^{-1}$ flows through the classrooms into the atrium before leaving the building through the atrium roof windows. The assumed direct air change between atrium and ambience amounts to $2300 \text{ m}^3\text{h}^{-1}$. The air change in the atrium determined for the calculation and related to the atrium volume of 4600 m^3 thus comes to 2.4 h^{-1} related to the total volume of the two atria. The ventilating strategies for winter and for summer are shown in Figure 7.3.2.

The heating energy demand that was calculated with the dynamic simulation program for the school building prior to retrofitting amounts to 212 kWh/m²a. By the energetic retrofitting of the external walls - except the wall adjoining the courtyard - and of the windows and the roof as well, the heating energy demand can be reduced by 99 kWh/m²a to 113 kWh/m²a. The courtyard glass roof, of low-E coated glazing, reduces the heating energy demand to 68 kWh/m²a. With a heated area of 3807 m², this corresponds to a saving of about 171 MWh. This calculation is done on the basis that the classrooms are not ventilated through the atrium. However, if part of the ventilation is done through the atrium, as described above, 5 kWh/m²a of the heating energy demand can be saved in addition.

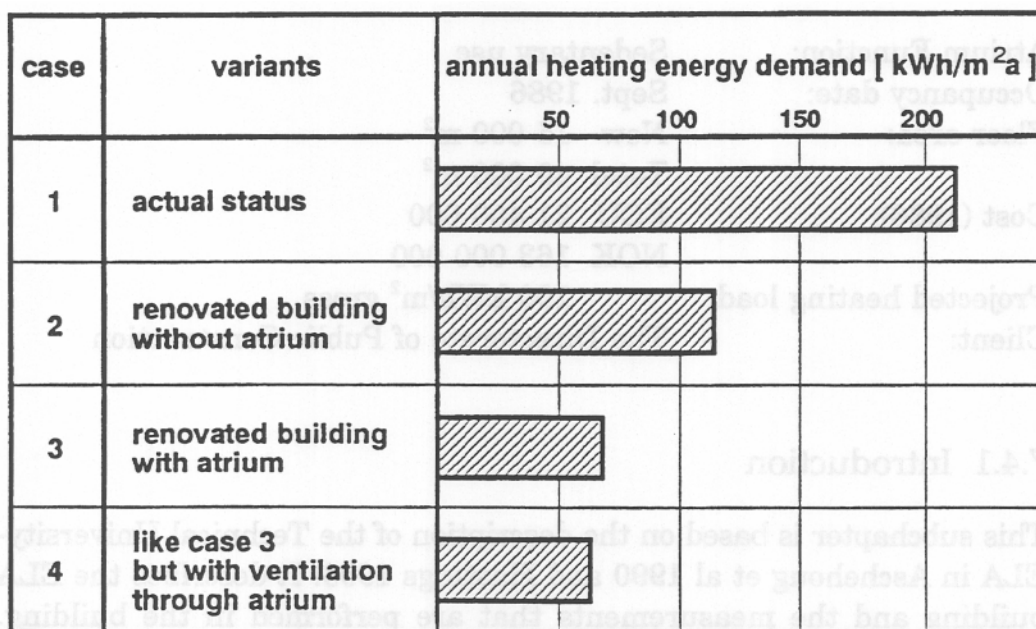


Figure 7.3.4: Annual heating energy demand of the school building prior to retrofitting and for different energy conservation measures.

For a graphical representation of the various calculated options of heating energy demand rates see Figure 7.3.4.

extension project includes offices for faculty and researchers, smaller seminar rooms and exercise labs, light electronics and computer labs, a multi-storey high voltage lab, and a cafeteria. New auditoria were also built, by reconstruction of existing lab facilities.

The extension consists of three new parallel four storey rectangular blocks and four linear shaped atria, filling out the spaces between these and existing buildings.

Table 7.4.1 Climate

October - April:		Annual:	
Degree days: (base 20°C)	4180	Degree days:	5510
Global solar hor.kWh/m ² :	220	Global hor.kWh/m ²	810
Sunshine hours:	470	Sunshine hours:	1350
Relative sunshine:	0.25	Relative sunshine:	0.30
		Average temp.°C:	4.9
		Design temp.°C:	-19

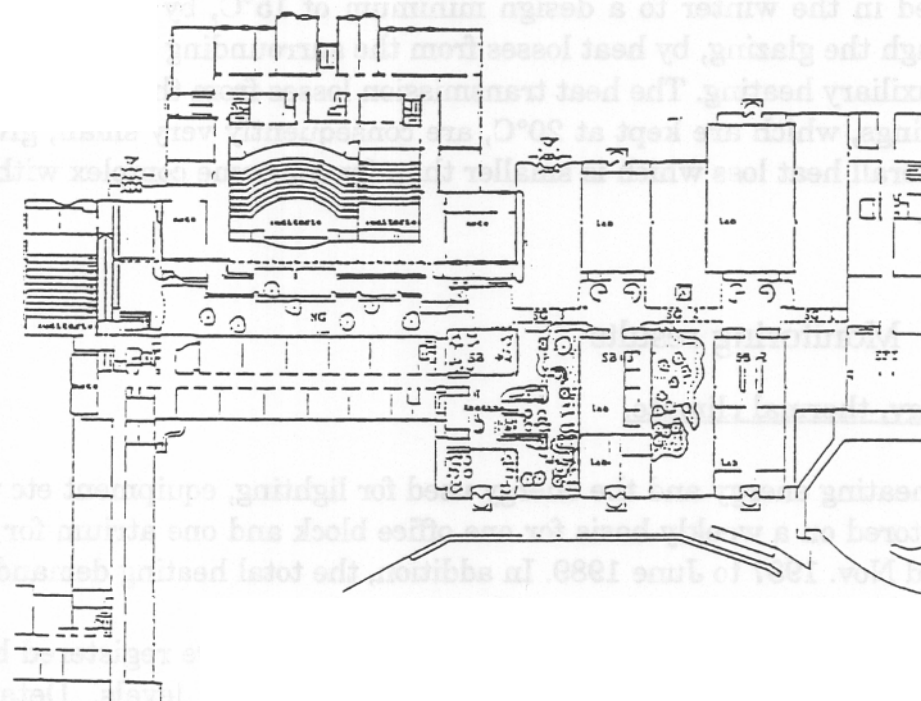


Figure 7.4.1 Ground level plan for the new building complex.

The new buildings are constructed of precast concrete columns, beams, and hollow core slabs, with steel frames as structural support for the atrium glazing. The exterior walls are insulated concrete sandwich panels, with double glazed low-emissivity windows. The intermediate

result of user demands. The atrium spaces were intended to be used for circulation and temporary occupancy only, but because of the general over-crowding of students in the complex, they now use the atria as general study places, which require a higher temperature for thermal comfort. Consequently, the atria heating demand has also risen steadily in the period, while the office heating energy is somewhat reduced, as the transmission losses to the atria now are almost zero.

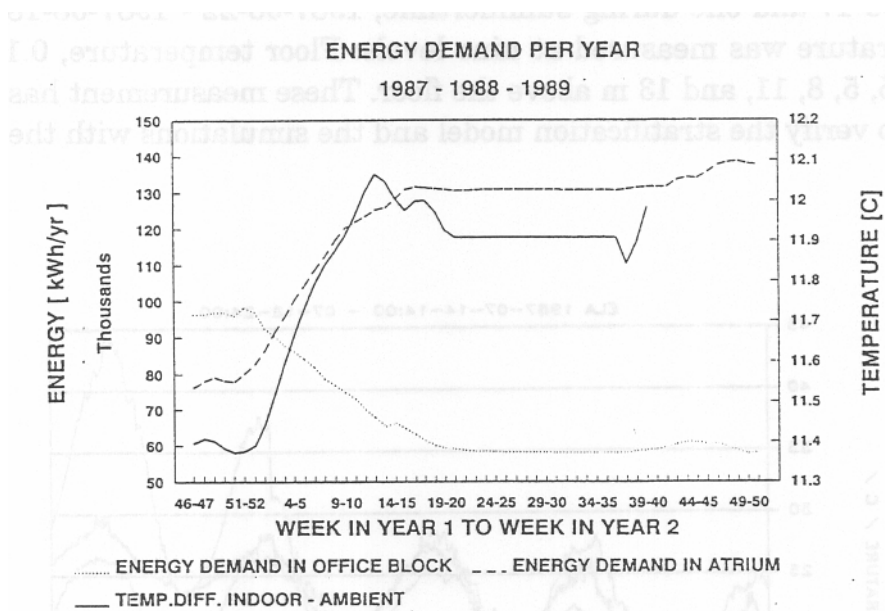


Figure 7.4.2 Trends in the annual heating load in one atrium and one office block.

Table 7.4.3 Energy use in kWh/m²

	Monitored in ELA	Norwegian Universities Average	NS3031 New Office	New laboratory
Office block: - lights, equipm: - heating:	67 41			
Atrium: - heating:	148			
Office block +atrium: - heating: - total:	60 127	270	90-130	150-250

inaccurate, as the mixing fan capacity was inadequate.

Some measurements were also carried out without mixing fans, in order to trace the air flow patterns in the atrium with hatches closed. These showed that the lower part of the atrium had the cleanest air, and that the upper part functioned as an air outlet; an air flow pattern similar to displacement ventilation.

Occupant opinions

The occupants' reactions to thermal comfort, air quality, and daylighting were also obtained in a comprehensive survey. Some major conclusions are:

- There are many complaints about high temperatures and poor air quality in offices facing the atria. Occupants are on the whole satisfied with conditions in the atria themselves. Daylight levels in the offices are considered adequate, but artificial lighting is kept on all year.
- The rating, on linear attribute scales, is quite similar to the rating given the University Center at Dragvold (Subchapter 6.3.13).
- Noise levels in the atria and noise disturbance from the atria to the office spaces also give rise to some complaints.

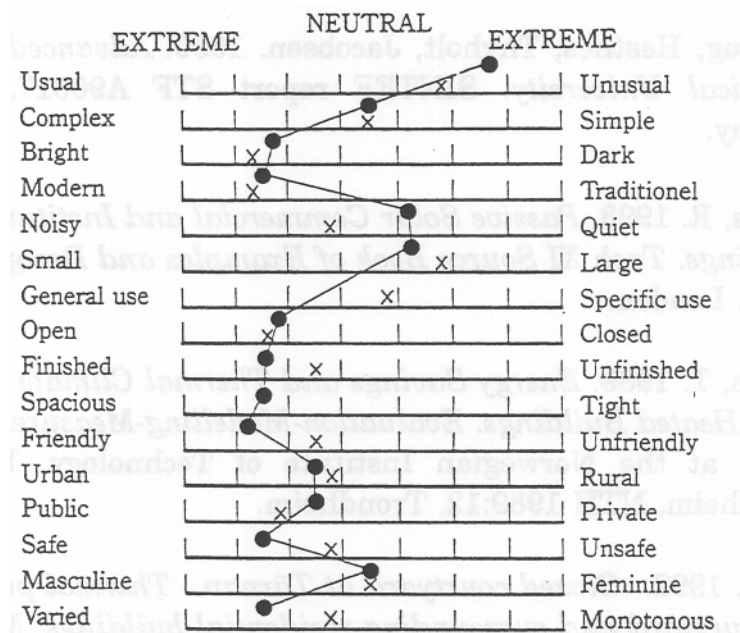


Figure 7.4.4 Occupant rating of the ELA building and the Dragvold University on a seven point scale. ● = Dragvold, X = ELA.

8. The use of CFD in the task XII

8.1 Introduction

Computational fluid dynamics - CFD seems to be a very promising tool in the design process for atria and other large rooms. The continuous development of computer technology and software and the decreasing costs for computing, makes the CFD a must for future design.

CFD-simulations seem to have the most cost-effective use for verification of indoor environment and for trouble shooting. That is for the last stage in the design process before construction. At previous stages in the process, when information is more scarce, experience and simpler tools should be used to keep costs at a low level.

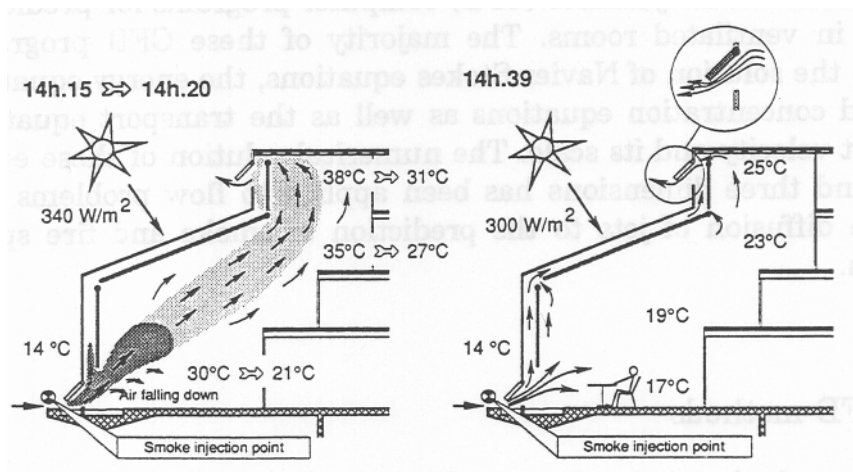
The use of CFD-codes was some years ago limited to experts in fluid dynamics and numerical methods. And those experts mostly computed idealized model-problems to test methods more than to solve engineering problems. Today, user-friendly commercial CFD-programs are offered - there are even special versions for ventilation of rooms. Though, there is still a need for expert knowledge to achieve realistic and accurate solutions from CFD-programs.

The most common CFD-codes include good turbulence models and are capable of giving computational results as good as needed for most engineering purposes. However, realistic results are still dependent on user-knowledge and on computer resources. The user-knowledge needed to simulate indoor climate and energy consumption is a mix of knowledge from HVAC and fluid dynamics with elements from numerical methods and architectural and civil engineering.

The objective of this chapter is on one hand to explain why CFD has been used in the Task 12 and in the other hand to bring attention to and to give guidance to the most essential factors in achieving a realistic and accurate solutions from CFD-simulations of atria.

8.1.2 CFD used in atrium calculations

- The use of CFD is not strictly limited to steady cases, but as it is a time consuming (calculation) simulation tool, so we will use it only in steady condition. This is not too important because normally the atrium structure is light.
- Example of an unsteady case (Nuni); sudden opening of hatches.



Unsteady measurements

- The results of CFD calculation are good in comparison to measurements, if the boundary conditions are sufficiently well defined:

→ 4 The one of the experiment should be known

4 It should be possible to introduce these boundary conditions in the calculations in the right way, this subject will be treated in chapter 3.

- Example of useful informations received from CFD

Temperature field (Comfort, stratification, energy)

Velocity field (Comfort, air exchange rate)

Down draft problems (Comfort)

- Wind influence

The CFD are not a concurrent tool of building dynamic simulation programs but are a complementary, it can be used as an "experiment" to calculate ("mesure") values we need to develop and evaluate simplified models.

Finally, the CFD can also be used for planning measurements with a coarse mesh (or modelling) of the space it is already possible to find the most convenient place to put the sensors.

Momentum (Navier-Stokes) equations :

$$\frac{\partial u_i}{\partial t} + u_j \frac{\partial u_i}{\partial x_j} = (\nu + \nu_t) \frac{\partial^2 u_i}{\partial x_j^2} + g_i (\rho - \rho_0) - \frac{1}{\rho} \frac{\partial p}{\partial x_i} \quad (2)$$

transient convection diffusion bouyancy pressure
term term term term gradient

Energy equation :

$$\frac{\partial T}{\partial t} + u_j \frac{\partial T}{\partial x_j} = (\alpha + \alpha_t) \frac{\partial^2 T}{\partial x_j^2} + \frac{q'''}{\rho c_p} \quad (3)$$

transient convection diffusion source
term term term term

$$\frac{\partial k}{\partial t} + u_j \frac{\partial k}{\partial x_j} = \left(\nu + \frac{\nu_t}{\sigma_k} \right) \frac{\partial^2 k}{\partial x_j^2} \quad (4)$$

$$+ \nu_t \left(\frac{\partial u_i}{\partial x_j} + \frac{\partial u_j}{\partial x_i} \right) \frac{\partial u_i}{\partial x_j} - \beta g_j \frac{\nu_t}{\sigma_t} \frac{\partial T}{\partial x_j} - C_D \varepsilon$$

$$\frac{\partial \varepsilon}{\partial t} + u_j \frac{\partial \varepsilon}{\partial x_j} = \left(\nu + \frac{\nu_t}{\sigma_\varepsilon} \right) \frac{\partial^2 \varepsilon}{\partial x_j^2} \quad (5)$$

$$+ \frac{\nu_t C_1 \varepsilon}{k} \left(\frac{\partial u_i}{\partial x_j} + \frac{\partial u_j}{\partial x_i} \right) \frac{\partial u_i}{\partial x_j} - \frac{C_2 \varepsilon^2}{k}$$

u_i represents velocities and x_i represents coordinates in tensor notation while t represents time and p is density of the fluid. T and p represents temperature and pressure, respectively. ν is the kinematic viscosity, α is the thermal diffusivity coefficient C_p specific heat and (β is the volumetric expansion coefficient of the fluid. q''' represents the heating power of a local heat source.

Eq.(3) ensures conservation of energy of each small volume of the flow field. The first term on the left-hand side represents the increase in energy by temperature-increase with time for the fluid in the element. The other three terms account for the net convection of heat into the fluid element. The right-hand terms describes heat conduction and heat sources.

Eq. (4) is a transport equation for turbulent kinetic energy. The terms on the right-hand side represents diffusion, production by velocity gradients and by temperature gradients and dissipation of turbulent kinetic energy.

Eq. (5) is a transport equation for dissipation rate of turbulence.

The equations above can be characterized as a set of coupled non-linear partial differential equations of second order. The equations are of elliptic type. This entails boundary conditions be given for the dependent variables on all parts of a continuous boundary enveloping the flow problem.

During the computation, the dependent variables are solved. Results are expressed as velocity components, turbulent kinetic energy and temperature for each grid or cell in the flow field.

8.2.3 Wall functions

Close to the wall the transport equations do not apply because of the dumping effect of the wall. In that region CFD programs must use algebraic equations called wall function. This approach does not require an ultrafine grid near the surface, so that it also contribute in saving calculation time. This approach will be discussed more in detail in chapter 8.3.

8.2.4 Solution of the transport equation

The general transport equation

The transport equations for momentum, temperature, concentration and the turbulence scales k and c and all have the general form :

$$\frac{\partial}{\partial t} (\rho\phi) + \text{div} (\rho V\phi - \Gamma_{\phi} \text{grad}\phi) = S_{\phi} \quad (8)$$

transient + convection - diffusion = source

where

In order to establish a more relevant parameter, the PPD-index was introduced. The PPD predicts the percentage of dissatisfied persons of a large group. The value for the PPD-index is directly dependent on the value of the PMV-index. It is recommended that the PPD be lower than 10 % to achieve sufficient thermal comfort in indoor environments. That corresponds to $-0.5 \leq \text{PMV} \leq +0.5$.

Mathematical expressions for the PMV- and PPD-indices are given in the ISO 7730.

The activity level of a person is expressed by a value for metabolism, and the thermal insulation of clothing is expressed by a clo-value. These values be set according to planned use of the atrium.

Air temperature and air velocity in every location in the zone of occupancy can be found by performing CFD-simulations for the atrium.

Then there is only one unknown value left to calculate the PMV. That is the value for mean radiant temperature. That value has to be computed by calculating the net exchange of radiation between a person and the surroundings. Generally, a lot of information on geometry and radiation properties for different surfaces have to be specified. A somewhat idealized approach for mean radiant temperature calculation is suggested by Tjelflaat. Calculations are based on the assumption that the atrium is empty except from one person that be placed in any location in the zone of occupancy.

Satisfying general thermal comfort is the most important issue. However, it is also important to evaluate local discomfort for people being in a sedentary position.

Draught is often causing local discomfort and is defined as heat loss by convection from parts of the body to the room air. Air speed and air temperature are the most important factors but it has been found that velocity fluctuations may enhance heat loss considerably. Draft has been considered and discussed by Fanger, and later his co-worker Melikow has given an extensive review of the field and a model for draft risk DR has been developed.

The percentage dissatisfied due to draught is given by:

$$DR = (34 - t_a) (v - 0.05)^{0.62} (0.37v \cdot Tu + 3.143) \quad (9)$$

where v is set equal to 0.05 m/s for $v < 0.05$ m/s and DR is set equal to 100% when DR is calculated to be larger than that.

KAMELEON-II is developed to solve the equations in general orthogonal coordinates. However, only Cartesian, cylindrical and spherical coordinate systems are included with the code. The Cartesian coordinates system is normally used to model ventilated rooms.

Flow boundary conditions at walls can be described as slip or non-slip conditions. Velocities and pressures must be described at inlets while zero-gradient in direction of flow is assumed for the variables at outlets.

The temperature of inlet flows must be given as boundary conditions. At walls, either the temperature or the heat flux must be prescribed.

Within the solution domain, closed or porous obstacles and heat- and contaminant sources and sinks can be modeled to simulate ventilated rooms realistically. An internal fan in the room can also be modeled by using a facility that can lock velocities for small areas within the flow field.

Numerical solution procedure

The finite-difference method is used to discretize the differential equations describing the problem. Three difference schemes are available by selection; the first order upwind-, the hybrid- and the power-law schemes. Normally, problems are first solved by using the upwind method as that is the most economical. The resulting set of algebraic equations is solved on a staggered grid.

To integrate the equations, a pressure correction method based on the simple algorithm is applied to iterate towards a converged solution. The use of 3 alternative improvements of the simple algorithm can be selected. The computational method is basically as described by Patankar (1980).

Three different matrix solvers are available; one for scalar processing computers and two for vector processing computers. One of the solvers for vector computers is for problems where the number of gridpoints is predominant in one direction.

A detailed description of the KAMELEON-II program can be found in Laksa and Vembe (1991).

Pre- and postprocessors

Lizard is a graphical preprocessor used to set up simulation cases for KAMELEON-II. Lizard runs on PCs and workstations. Monitor is a postprocessor used for graphical display of velocity- and temperature fields and for other parameters of interest.

8.2.7 Description of Flovent

Introduction

Flovent is a special-purpose computational fluid dynamic (CFD) program which has been conceived, specified and developed by collaboration between Flomerics Ltd and BSRIA (building serviced research and information association : UK). Flovent is a practical tool meeting the needs of the designers of heating, ventilation (mechanical or natural ventilation) and air-conditioning systems for building. This program is commercially available.

Problem formulation

Flovent is capable of solving the same general flow problems presented in the KAMELEON description. As Flovent is using similar turbulence model and numerical solution procedure as KAMELEON, it is not useful to repeat here this introduction. We will simply point out the principal differences with KAMELEON.

Only cartesian coordinates are available in Flovent

At wall either the temperature, or the temperature and the heat coefficient transfer or the heat flux can be specified.

The thermal effect (inertial) of the wall can be taken into account although it is time consuming (unsteady calculation).

The infra red radiation can be modelled between two different surfaces.

Calculation procedures for thermal environment parameters as comfort have been developed, but not air quality values are available directly from the results (they must be put processed).

•

8.2.8 Limitations

CFD are limited in different directions and need to be improved in the following areas :

The need for a universal turbulence model which is valid near walls and at predominant Reynolds-numbers in the core of the enclosure.

- Need for more accurate prediction of natural and mixed convection at cold or warm surfaces.
- Need for improved modelling of supply jet devices.
- Need for improved computational grid. - Problems with number and size of grid cells and difficulty of achieving grid-independent solutions; especially for large enclosures.
- Need for improved numerical procedure to reach solution of system of finite-difference equations. - It can be difficult or slow to achieve converged solutions, especially for large enclosures with buoyant flow.
- Need for addition of radiation modelling to CFD codes.
- Need for knowledge of the interaction of the airflow with thermal building dynamics.

That said, significant advances in the above areas have been made. Many investigators (Murakami & Kato 1989; Whittle 1991; and others) have argued that common CFD codes are already capable of predicting room air movement with sufficient realism to be of use in design practice, despite their shortcomings.

The second issue is that a high degree of engineering judgement and experience is needed to apply CFD to actual buildings, and achieve realistic solutions. The user must have knowledge from the fields of HVAC and fluid dynamics, with elements from numerical methods as well as architectural and building engineering. There is therefore a need for guidelines for the use of CFD.

•